



Title	Molecular mechanism of root development regulated by trafficking pathway via TGN/EE
Author(s)	松浦, 友紀
Citation	大阪大学, 2021, 博士論文
Version Type	VoR
URL	<a href="https://doi.org/10.18910/82028">https://doi.org/10.18910/82028</a>
rights	
Note	

*The University of Osaka Institutional Knowledge Archive : OUKA*

<https://ir.library.osaka-u.ac.jp/>

The University of Osaka

**Molecular mechanism of root development  
regulated by trafficking pathway via TGN/EE**

(トランスゴルジ網における膜交通が支える

根の発生制御の分子機構)

Department of Biological Sciences,  
Graduate School of Science,  
Osaka University

Yuki Matsuura

## **Table of contents**

Abstract -----	1-2
Introduction-----	3-6
Results-----	6-15
Discussion-----	16-19
Materials and Methods-----	20-23
Acknowledgements-----	24
References-----	25-30
Figures-----	31-57

## Abstract

Membrane trafficking at *trans*-Golgi network (TGN/EE) is crucial for correctly distributing various membrane proteins to their destination. Polarly localized auxin efflux proteins, including PIN-FORMED1 (PIN1), are dynamically transported between the endosomes and the plasma membrane (PM) in the plant cells. PIN auxin efflux proteins exhibit asymmetric distribution at the plasma membrane (PM) and collectively play pivotal roles in generating local auxin accumulation, which underlies various auxin-dependent developmental processes. Polar auxin transport is involved in multiple aspects of plant development, including root growth, lateral root branching, embryogenesis, and vasculature development.

Some membrane trafficking factors involved in PIN transport were isolated. The intracellular trafficking of PIN1 protein is sensitive to the fungal toxin brefeldin A (BFA), which is known to inhibit guanine nucleotide exchange factors for ADP ribosylation factors (ARF GEFs) such as GNOM. In a previous study, an Arabidopsis mutant *BFA-visualized endocytic trafficking defective 1* (*ben1*), *ben2*, and *ben3* which exhibited reduced sensitivity to BFA in terms of BFA-induced intracellular PIN1 agglomeration were isolated. And it has been revealed that each causal gene was endosomal trafficking components BEN1/BIG5 (ARF GEF), BEN2/VPS45 (Sec1/Munc18 protein), and BEN3/BIG2 (ARF GEF). Mutations in both BEN1 and BEN2 resulted in defects in polar PIN localization, auxin response gradients, and in root architecture.

In this study, I have attempted to gain insight into the developmental roles of these trafficking components. I showed that while genetic or pharmacological disturbances of auxin distribution reduced dividing cells in the root tips and resulted in reduced root growth, the same manipulations had only moderate impact on *ben1; ben2* double mutants. In addition, I established transgenic lines in which BEN2/VPS45 is expressed under control of tissue-specific promoters and demonstrated that BEN2/VPS45 regulates the intracellular traffic of PIN proteins in cell-autonomous manner, at least in stele and epidermal cells. Furthermore, BEN2/VPS45 rescued the root architecture defects when expressed in internal tissues of *ben1; ben2* double mutants. These results corroborate the roles of the endosomal trafficking component BEN2/VPS45 in regulation of auxin dependent developmental processes, and suggest that BEN2/VPS45 is required for sustainable root growth, most likely through regulation of tip-ward auxin transport through the internal tissues of root.

To assess the function of BEN3 in PIN trafficking, I examined whether de novo synthesized PIN1 protein was targeted to PM by BEN3, and revealed that BEN3/BIG2

had a crucial role for this BFA-sensitive PIN trafficking from TGN/EE to PM. Taken together, these results suggest that BEN3/ BIG2 is an ARF GEF component, which confers BFA sensitivity to the TGN/EE in Arabidopsis.

In addition, it is known that SNARE protein regulates Sec1/Munc18 protein, and that BEN2 binds with SYP4 SNARE protein. Consistent with their interaction and common localization, *syp42; syp43* double mutant shows short primary root and a lot of lateral root (Uemura et al., 2012). To investigate the functional relationship between SYP4 and BEN2, I generated the *syp42; syp43* expressing SYP43 tissue-specifically. Unlike BEN2 which showed distinct expression pattern under the control of each promoters in *ben1; ben2*, SYP43 showed the expansion of fluorescent signals to the neighboring tissue layers. Furthermore, all lines of these transgenic lines showed the recovered root architecture. This suggested that the expression of GFP-SYP43 was not restricted strictly or SYP43 moved intercellularly after translation, and this was sufficient to recover the root growth defects in the *syp42; syp43* mutants.

To get new insights of membrane trafficking in root development, I focused on the effect of environmental factors in root development. In this research, it was demonstrated that *ben1; ben2* is less sensitive to phosphate starvation. And to know whether in *ben1; ben2* on the media including phosphate the response to phosphate starvation occurs, I visualized the iron deposition which reflect phosphate starvation. This revealed that iron deposition was enhanced in *ben1; ben2* in spite of the presence of phosphate, suggesting that the defects of PIN polarity caused by the mutation in *BEN1* and *BEN2* also affects the signaling involved in phosphate starvation or that the receptor for the concentration of phosphate and/or transporter is misregulated in *ben1; ben2*.

In conclusion, it was demonstrated that some membrane trafficking factor located in TGN/EE, BEN1, BEN2, BEN3, and SYP4, is involved in root development through the PIN transport. However, the molecular mechanism and the responsible tissue for regulation of root architecture is distinct respectively.

## Introduction

Plant hormone auxin is involved in multiple aspects of plant growth and development, such as embryonic patterning, formation of lateral organs, regulation of organ growth, and tropic responses (Mockaitis and Estelle, 2008; Vanneste and Friml, 2009; Grunewald and Friml, 2010; Zwiewka et al., 2019). Auxin-dependent developmental regulation largely relies on local auxin gradient, which is generated by local auxin biosynthesis, polar transport, and/or degradation (Vanneste and Friml, 2009; Casanova-Sáez and Voß, 2019). Root system plays physiological roles such as assimilation and transport of nutrients, and therefore, its architecture is an agriculturally important trait. Root system architecture (RSA) is typically determined by the extent of root growth and branching patterns, which are plastically modulated by external stimuli. Transport and local accumulation of auxin play pivotal roles in regulating both root growth and branching patterns. While certain level of auxin is required for root growth, excess amounts of auxin strongly inhibit root elongation, and promote lateral root initiation and emergence (Petricka et al., 2012; Sugawara et al., 2015; Banda et al., 2019). Auxin is mainly synthesized in young leaves and root tip, and shoot-driven auxin is transported through vasculature toward root tip (Ljung et al., 2005). At the root tip, auxin flux is redirected shootwards through the outer layer of tissues such as epidermis, cortex, and lateral root cap. This auxin flow depends on auxin influx and efflux transporters. Several classes of auxin transport proteins, including PIN-formed (PIN) family protein and AUXIN/LIKE AUX1 (AUX/LAX) family protein, have been isolated. Of these, PIN family auxin-efflux proteins are expressed widely in plant tissues, and some are localized to the plasma membrane (PM) with polar distribution and play a critical role in intercellular transport of auxin. Polar localization of PIN proteins is consistent with the known directionality of auxin transport (Tanaka et al., 2006) and in some cases, manipulation of PIN polar localization causes changes in auxin distribution (Wiśniewska et al., 2006; Huang et al., 2010), indicating the biological significance of the polar localization of PIN proteins in regulating auxin distribution.

In *Arabidopsis*, PIN1, 2, 3, 4, and 7 are localized at the PM (Grunewald and Friml, 2010). PIN1 is expressed in internal tissues in the root tip, and localized at the basal side of the PM. On the other hand, PIN2 is expressed in outer tissues, including epidermis, cortex, and lateral root cap, and is typically localized to the apical side of the epidermal cells. PIN3, 4, and 7 are expressed in the vasculature and columella cells. Members of PIN proteins have auxin efflux activity and expressed in partially overlapping patterns

(Vanneste and Friml, 2009; Sauer and Kleine-Vehn, 2019). Due to their partial redundancy, the single mutants display specific defects in shoot organ formation, gravitropic defects or moderate patterning defects, whereas the multiple mutants exhibit remarkable inhibition of root architecture (Friml et al., 2003; Blilou et al., 2005; Vieten et al., 2005). The developmental defects of the *pin* mutants correlate with auxin distribution defects, which are consistent with the polar localization of corresponding PIN proteins at the PM, suggesting that PIN dependent auxin transport plays essential roles in multiple developmental processes.

The polar localization of the PIN proteins at the PM requires post-translational modification of PIN proteins and membrane trafficking (Zwiewka et al., 2019; Zhang et al., 2020). For instance, in the root vascular tissues, PIN1 proteins are reversibly accumulated in endosomes and depleted from the PM upon treatment, when seedlings are treated with the vesicle transport inhibitor brefeldin A (BFA) (Geldner et al., 2003; Zwiewka et al., 2019). This indicates that PIN1 is constitutively transported by endocytosis and recycled back to the PM. Many membrane trafficking factors related to this trafficking have been isolated. GNOM ARF GEF is a prominent target of BFA in terms of PIN1 recycling to the PM and is required for localization of PIN1 at the basal side of the vascular cells (Geldner et al., 2003; Kleine-Vehn et al., 2008). In addition, ARF GEF interacting proteins such as ARF1 and Aminophospholipid ATPase3 (ALA3) play essential roles in the localization of PIN proteins at the PM (Tanaka et al., 2014; Singh et al., 2018; Zhang et al., 2020). BFA treatment induces the formation of agglomerated membrane compartments, where most of GNOM proteins accumulate. It is believed that endocytosed vesicles rapidly reach the trans-Golgi network which is equivalent to early endosome in plants (TGN/EE). BFA compartments are characterized by accumulation of many TGN/EE-related markers and therefore endocytosed as well as newly synthesized PM cargo proteins accumulate there. As such, it is hypothesized that BFA inhibits the trafficking from the TGN/EE in Arabidopsis. However, in the normal condition, majority of GNOM proteins are detected at the Golgi apparatus and at the PM, but not from the TGN/EE (Naramoto et al., 2014) and the molecular mechanism underlying trafficking and polar localization of PIN proteins is not fully understood.

In previous study, Arabidopsis mutants designated as *bfa-visualized endocytosis defective1* (*ben1*), *ben2*, and *ben3* mutants, have been isolated, which exhibited less pronounced PIN1-GFP accumulation at the BFA compartment by a fluorescence imaging-based forward genetic screening (Tanaka et al., 2009). *BEN1* and *BEN3* encode ARF GEF

BIG5 and BIG2 (Tanaka et al., 2009), which activates ARF GTPases promoting membrane budding (Singh et al., 2018). *BEN2* encodes a Sec1/ Munc18 protein VPS45, which interacts with SNARE protein to promote membrane fusion (Tanaka et al., 2013). *BEN1*, *BEN2*, and *BEN3* proteins localized to the TGN/EE and are speculated to functions in recycling of PIN protein. Mutation in either *BEN1* or *BEN2* moderately affects trafficking and polar localization of PIN proteins, but does not cause severe developmental defects. On the other hand, *ben1; ben2* double mutant shows pleiotropic defects including short primary root, excess number of lateral roots, and small shoot (Figure 1A). However, detailed molecular mechanism by which *BEN1*, *BEN2*, and *BEN3* regulate root architecture still remain to be elucidated.

Sec1/Munc18 protein is regulatory factor for SNARE protein. It is known that *BEN2* binds with SYP4 SNARE protein. The SYP4 group (*SYP41*, *SYP42*, and *SYP43*) localizes on the TGN and has redundant functions. Especially *syp42; syp43* double mutant shows short primary root and a lot of lateral root (Uemura et al., 2012). Based on the common points between SYP4 and *BEN2*, it was suggested that SYP4 also has crucial role for root development through the regulation of auxin distribution like *BEN2*.

In addition to endogenous plant hormone, environmental factors also affect root development. It is known that the nutritional condition in soil has great influence to root architecture (Ericsson, 1995). Particularly, the deficiency of phosphate inhibits the elongation of primary root and promotes lateral root formation (Péret *et al.*, 2011), which resemble to the root architecture of *ben1; ben2*. The deficiency of phosphate induces the increase of iron availabilities, causing callose deposition in meristematic region (Müller et al., 2015). Excess callose deposition inhibits intercellular communication, and intercellular signaling has crucial role to regulate cell division and differentiation (Gallagher et al., 2014; Perilli et al., 2012). These findings raised a question whether *BEN1* and/or *BEN2* are involved in response pathway to phosphate starvation.

In this study, I investigated the regulation mechanism for root development mediated by membrane trafficking. I attempted to dissect the role of the endosomal component *BEN2/VPS45* in regulating PIN trafficking and root development. I showed that the meristematic activity is reduced in *ben1; ben2* double mutant and the root growth of the double mutants were relatively insensitive to genetic or pharmacological manipulation of auxin transport and synthesis. Furthermore, tissue-specific rescue experiments demonstrated that, while *BEN2/VPS45* regulates intracellular trafficking of PIN1 and

PIN2 in cell autonomous fashion, it is mainly required in internal tissues to promote root growth. In addition, I demonstrated that BEN3/BIG2 also functions for PIN trafficking from TGN/EE to PM. This indicates that BEN1 and BEN3 have redundant localization and functions. On the other hand, SYP4 was appeared not to have tissue-specific functions for root development, suggesting that BEN2 was more promising target involving in membrane fusion which was affected by environmental stimuli to adapt root architecture finely. On behalf of environmental stimuli, response to phosphate starvation was appeared to be enhanced in the defects of *BEN1* and *BEN2*. In conclusion, my study implies that membrane trafficking factors involved in the transport from TGN/EE to PM function for root development, which is regulated by tissue-specifically or not, respectively.

## Results

### 1. Developmental defects in *ben1; ben2*

#### 1-1. *ben1; ben2* shows defects of auxin distribution

To visualize the auxin distribution, I observed the root tips and pericycle which are responsible to root length and lateral root formation in WT and *ben1; ben2* using auxin-responsive reporter DR5::GFP. In WT, DR5::GFP was detected in the root tip and ectopically in pericycle where prospective lateral root primordia is formed. On the other hand, in *ben1; ben2*, DR5::GFP was detected widely in pericycle (Figure 2). This indicates that auxin distribution in *ben1; ben2* is disrupted.

#### 1-2. Activity of the root meristem is reduced in *ben1; ben2*

Reduced growth of the primary root is an obvious phenotype of the *ben1; ben2* double mutant seedlings (Figure 1A). To investigate the developmental basis of the root growth inhibition, first I analyzed the meristematic activity of wildtype, *ben1*, *ben2*, and *ben1; ben2* seedling roots. In the wild-type root, relatively small cells with high cell division capacity represent the zone of cell division, or the root meristem, which locates above the quiescent center (QC). *ben1* and *ben2* single mutants showed similar size of meristem and number of cells in meristematic regions compared with wildtype, although *ben2* single mutant had a tendency to have slightly short root meristem. On the other hand, in the *ben1; ben2* double mutants, the size of root meristem and the number of cells in the meristematic regions were reduced as compared with wildtype root (Figures 1B–D).

Next, to confirm whether excess lateral root inhibit root elongation in *ben1; ben2*, I crossed *slr* mutant which does not form lateral root (Fukaki et al., 2002) with Col-0, *ben1*, *ben2*, and *ben1; ben2* and quantified the root length. In Col-0, *ben1*, and *ben2*, the mutants which did not form lateral root did not show the recovery of root length. Interestingly, *ben1; ben2* which did not form lateral root show the reduction of root length (Figure 3A, B). This suggests that in *ben1; ben2* the short primary root is not caused by excess lateral roots.

These results suggest that cells ongoing cell proliferation at the root tip were decreased in *ben1; ben2*, which could at least in part account for the root growth inhibition in the mutants.

#### 1-3. *ben1; ben2* double mutant is less sensitive to genetic manipulation of PIN expression and pharmacological inhibition of auxin biosynthesis

In a preceding study, it was indicated that BEN1 and BEN2 function in membrane

trafficking of PIN protein (Tanaka et al., 2009). However, it has remained elusive whether the developmental defects observed in *ben1; ben2* double mutants are caused by the abnormality of PIN-dependent auxin distribution. To gain insight into the causal relationship between the growth defects of the *ben1; ben2* double mutants and functionality of PIN proteins and/or auxin distribution, I next tested the genetic relationship between the *ben1; ben2* double mutant and PIN1 overexpression, which is known to affect root growth and meristem size (Mravec et al., 2008). To overexpress PIN1 in the mutant background, an estradiol-inducible PIN1 (XVE-PIN1) was introduced into the *ben1*, *ben2*, and *ben1; ben2* mutants. Transcription of *PIN1* is induced by adding  $\beta$ -estradiol. As reported previously, in wildtype background, the root length was dramatically reduced by overexpressing PIN1 (Figures 4A, B). Similarly, *ben1* single mutant showed reduction of root length. On the other hand, in *ben2* and *ben1; ben2* seedlings, growth of the primary root was only moderately inhibited, suggesting that root growth of the double mutant was less sensitive to the overexpression of PIN1 (Figures 4A, B).

I further investigated the effect of an auxin biosynthesis inhibitor kynurenine (kyn) on root growth of wildtype, *ben1*, *ben2*, and the *ben1; ben2* mutant seedlings. In wildtype, kyn clearly reduced the root length at 10  $\mu$ M by 50% on average as compared with DMSO control (Figures 4C, D). In contrast, root length of the *ben1*, *ben2*, and *ben1; ben2* mutants was reduced by 30%, 20%, and 30% at 10  $\mu$ M kyn respectively, indicating that the root growth of the mutant was only mildly inhibited by kyn (Figures 4C, D). Based on these observations, I reasoned that the defects of root development in *ben1; ben2* is, at least to some extent, caused by the change of PIN- and auxin-dependent regulation of root meristem and BEN2 might play a particularly important role in regulating PIN-dependent root growth.

## **2. Tissue-specific function of BEN2**

### **2-1. BEN2/VPS45 is expressed throughout root and functions cell autonomously in PIN trafficking**

I focused on BEN2 function to form root architecture as *ben2* single mutant showed different response against PIN1 overexpression although *ben1* single mutant showed almost same response as seen in wildtype. BEN2 is expressed widely in root tip (Figure 5A). To test if BEN2 functions cell-autonomously in regulating PIN trafficking, I established transgenic lines which expressed BEN2 tissue-specifically in *ben2* single mutant background. For this purpose, BEN2 was expressed as GFP fusion protein under the control of either the *PHB* or *PIN2* promoters, which drives tissue-specific gene expression in internal tissues and outer tissues, respectively. Investigation of the GFP signals of the *pPHB::BEN2-GFP* and *pPIN2::BEN2-GFP* transgenic plants revealed tissue-specific expression, consistent with other reports (Vieten et al., 2005; Miyashima et al., 2011; Sebastian et al., 2015) (Figure 5B). By using these transgenic lines, *ben2* mutant phenotypes in terms of PIN trafficking was evaluated by using brefeldin A (BFA). It has been shown that, BFA inhibits exocytosis and induces accumulation of PIN1 and PIN2 proteins in the BFA compartments in wildtype cells, whereas the agglomeration of both PIN1 and PIN2 is less pronounced in *ben2* mutant cells (Tanaka et al., 2009; Tanaka et al., 2013). In transgenic lines, BFA compartments visualized with PIN1- and PIN2-antibody were pronounced only in the tissues where BEN2 proteins were supposed to express (Figures 5C, D). Together, these results imply that intercellular movement of BEN2-GFP fusion proteins is negligible, and indicate that BEN2-GFP rescued the intracellular PIN trafficking defects of the *ben2* mutant in cell-autonomous manner.

### **2-2. Expression of BEN2 in internal tissues is crucial for root architecture**

I next investigated the tissue-specific function of BEN2 on the root architecture. Because the *ben1* and *ben2* single mutant seedlings did not exhibit strong developmental defects, I chose *ben1; ben2* double mutants which exhibit clear morphological defects as the genetic background to express BEN2-GFP under control of tissue-specific promoters. For this experiment, I selected promoters to drive expression in internal tissues (*pPIN1* and *pPHB*), QC, cortex/endodermis initial (CEI) and endodermis (*pSCR*), and outer tissues (*pPIN2*) (Figure 6A). As judged by the overall morphology of the root system in young seedlings, *ben1; ben2; pPIN1::BEN2-GFP* and *ben1; ben2; pPHB::BEN2-GFP*, the root architecture was similar to *ben1* single mutant, indicating that expression of BEN2-GFP in the internal tissues significantly rescued the root growth defect (Figures 6B–E). On the contrary, in *ben1; ben2; pSCR::BEN2-GFP* and *ben1; ben2; pPIN2::BEN2-GFP*, the

growth defect of the primary roots did not recover (Figures 6B–E). These results indicated that BEN2 expressed in inner tissues has crucial role for root architecture.

### **2-3. Cell proliferation and auxin distribution in the tip of roots depend on BEN2 expressed in inner tissue**

To investigate the recovery mechanism of *ben1; ben2* by BEN2 expressed tissue-specifically, I introduced *CycB1;1-GUS* marker, which indicates the transition from G2 to M phase, into the mutants and transgenic lines. Under this condition, strong GUS signals were mainly detected in the cells within approximately 100 to 200  $\mu\text{m}$  above the QC in the *ben1* mutant background. In the *ben1; ben2* roots, however, the cells expressing GUS was confined in a smaller region, which was typically within less than 100  $\mu\text{m}$  above the QC (Figure 7A). These results suggest that *ben1; ben2; CycB1;1-GUS* shows reduction of cell proliferation compared with *ben1; CycB1;1-GUS*. The region expressing *CycB1;1-GUS* in root tip of *ben1; ben2; pPIN1::BEN2-GFP; CycB1;1-GUS* and *ben1; ben2; pPHB::BEN2-GFP; CycB1;1-GUS* was similar to that of *ben1; CycB1;1-GUS* (Figures 7A, B). On the other hand, *ben1; ben2; pPIN2::BEN2-GFP; CycB1;1-GUS* exhibited *CycB1;1-GUS* expression in confined regions close to the QC, patterns of which were indistinguishable from those observed in *ben1; ben2; CycB1;1-GUS* (Figures 7A, B). The pattern of GUS-positive cells of *ben1; ben2; pSCR::BEN2-GFP; CycB1;1-GUS* was intermediate of those observed in the *ben1* single mutant and *ben1; ben2* double mutant background, indicating that *pSCR::BEN2-GFP* moderately recovered the cell division activity in the root tip (Figures 7A, B).

To examine how the tissue-specific recovery of BEN2 affected the auxin response maxima, I introduced an auxin-response reporter *DR5rev::3xVenus-N7* in the mutants and transgenic lines. Characterization of Venus expression revealed that, while strong DR5 activity was detected in the root tip of *ben1* single mutant background in typical patterns, expression of *DR5rev::3xVenus-N7* was apparently reduced in the *ben1; ben2* double mutant background. Together with the results of previous observation of the patterns of *DR5rev::GFP* in the mutants (Tanaka et al., 2013), I reasoned that *ben2* mutation, in concert with *ben1* mutation, has affected auxin distribution and hence DR5 expression. The patterns of *DR5rev::3xVenus-N7* expression in the *ben1; ben2; pSCR::BEN2-GFP* and *ben1; ben2; pPIN2::BEN2-GFP* background were similar to those in *ben1; ben2* double mutant background, which showed narrow expression pattern at the tips of roots. In contrast, DR5 activity in the *ben1; ben2; pPHB::BEN2-GFP* background was similar to that in the *ben1* single mutant (Figure 7C). These results suggested that expression of BEN2 in the internal tissues including stele is relevant in auxin distribution at the root tip

and in sustaining cell proliferation.

#### **2-4. PIN Polarity depends on BEN2 expression**

To examine whether BEN2 expressed tissue-specifically regulates PIN polarity, I quantified PIN1 and PIN2 polarity in transgenic plants. PIN1 polarity defects in the stele of the *ben1; ben2* mutant roots were recovered in *ben1; ben2; pBEN2::BEN2-GFP*, *ben1; ben2; pPIN1::BEN2-GFP*, and *ben1; ben2; pPHB::BEN2-GFP*, in which BEN2 was expressed in inner tissues including stele. On the other hand, *ben1; ben2; pSCR::BEN2-GFP*, and *ben1; ben2; pPIN2::BEN2-GFP*, in which BEN2 was not expressed in inner tissues, exhibited obvious PIN1 polarity defects in stele, as seen in *ben1; ben2* double mutants (Figure 8A, B). Similarly, PIN2 polarity defects in epidermal cells were recovered in *ben1; ben2; pBEN2::BEN2-GFP* and *ben1; ben2; pPIN2::BEN2-GFP*, in which BEN2 was expressed in outer tissues. In contrast, the PIN2 polarity defects were detectable in *ben1; ben2; pPIN1::BEN2-GFP*, *ben1; ben2; pPHB::BEN2-GFP*, and *ben1; ben2; pSCR::BEN2-GFP* root epidermal cells, where BEN2 was not expressed (Figure 8C, D). These results indicate that BEN2 has a crucial role to regulate PIN1 and PIN2 polarity cell-autonomously.

#### **2-5. Resistance to auxin addition in *ben1; ben2***

To investigate whether the root growth defects in *ben1; ben2* are caused by lack of auxin in root tip, I treated seedlings with low concentration of auxin, 2,4-D. I observed alteration of auxin response distribution in each seedling with treatment of 2,4-D. In Col-0, *ben1*, and *ben2*, the pattern of auxin distribution did not change dramatically with 1 nM 2,4-D. And with 10 nM 2,4-D, they showed decreased auxin response around QC and increased auxin response in epidermis. On the other hand, in *ben1; ben2* treated with 2,4-D, the auxin response distribution expanded to columella root cap where in Col-0, *ben1*, and *ben2* auxin responses were detected but not in *ben1; ben2* without 2,4-D (Figure 9). This suggests that auxin distribution of *ben1; ben2* treated with 2,4-D resembles to that of Col-0, *ben1*, and *ben2* on normal medium. In *ben1; ben2; pPHB::BEN2-GFP*, the treatment of 10 nM 2,4-D caused the increase of auxin response in epidermis. On the other hand, in *ben1; ben2; pSCR::BEN2-GFP* and *ben1; ben2; pPIN2::BEN2-GFP*, auxin responses as visualized by *DR5::Venus-N7* fluorescence was slightly increased in QC with 2,4-D. And in *ben1; ben2; pPIN2::BEN2-GFP*, the slight increase of auxin in outer tissues was detected (Figure 9). This shows that BEN2 expressed in inner tissues has influence on the auxin distribution response to addition of 2,4-D around QC and outer tissues, and BEN2 expressed in outer tissues affects auxin pattern in outer tissues but not around QC.

Next, I measured the root length of seedlings. The treatment of 1 nM 2,4-D did not inhibit root elongation in all seedlings. However, in Col-0 and *ben1*, the root length was dramatically inhibited with the treatment of 10 nM 2,4-D. In *ben2*, the inhibition was more moderate. And in *ben1; ben2*, the root length was not significantly affected with the same treatment (Figure 10A, B). In *ben1; ben2; pPHB::BEN2-GFP*, the root length was inhibited with 10 nM 2,4-D. On the other hand, in *ben1; ben2; pSCR::BEN2-GFP* and *ben1; ben2; pPIN2::BEN2-GFP*, the decrease of root length was moderate compared with *ben1; ben2; pPHB::BEN2-GFP* (Figure 10A, B). This suggests that the addition of low concentration auxin did not inhibit root elongation in *ben1; ben2*, *ben1; ben2; pSCR::BEN2-GFP*, and *ben1; ben2; pPIN2::BEN2-GFP* which BEN2 was not expressed in inner tissues.

To investigate whether the activity of cell proliferation is affected by the treatment of auxin, I observed the pattern of CycB1;1-GUS. In Col-0, *ben1*, and *ben2*, with 1 nM 2,4-D, the expression pattern of CycB1;1-GUS did not change. With 10 nM 2,4-D, the region was decreased. On the other hand, in *ben1; ben2*, with 1 nM 2,4-D, the region expressing CycB1;1-GUS expanded compared with seedlings on the control medium (Figure 11). In *ben1; ben2; pPIN1::BEN2-GFP*, *ben1; ben2; pPHB::BEN2-GFP*, and *ben1; ben2; pSCR::BEN2-GFP*, the auxin activity was inhibited with 2,4-D. On the other hand, in *ben1; ben2; pPIN2::BEN2-GFP*, 1 nM 2,4-D slightly rescued the activity of cell proliferation (Figure 11). These results suggests that the addition of low concentration auxin could rescue the activity cell proliferation in *ben1; ben2* and *ben1; ben2; pPIN2::BEN2-GFP* but the recovery did not affect the root length.

## **2-6. The twist of root tip is rescued with BEN2 in inner tissues**

To investigate whether the mutations in *BEN1* and *BEN2* affect coordinated development of root cell files, I have characterized the shape of root tip, which typically exhibits straight cell files in wild type under our growth condition (Figure 12A). Morphological observations revealed that the primary root of Col-0, *ben1*, and *ben2* showed straight root tips. But almost all *ben1; ben2* double mutant seedlings exhibited twisted root tips. And this defect was recovered with the expression of *pBEN2::BEN2-GFP* and *pPHB::BEN2-GFP* (Figure 12B). This results suggest that the *ben1* and *ben2* mutations together might have caused uncoordinated tissue growths in root tip and BEN2 expressed in inner tissues affect not only inner but also outer cell files.

### **3. Other trafficking factors involved in root development**

#### **3-1. Multiple *ben3* alleles are associated with BFA-sensitive PIN1 trafficking**

In previous study, some *ben3* mutants were obtained and each responsible mutation was identified (Kitakura et al., 2017). To confirm the *ben3* mutants (*ben3-1*, *ben3-crisper*, *SALK-093944*, *SALK-024601*, and *SALK016558*), I checked the expression level of *BEN3* with RT-PCR. ... (Figure 13A, B). This indicated that in these *ben3* mutants *BEN3* did not function.

To investigate whether *BEN3* is involved in BFA-sensitive PIN1 trafficking like *BEN1* and *BEN2*, *ben3* mutants were treated with BFA. And BFA-body was immunostained with anti-PIN1 antibody. Col-0 showed BFA bodies with treatment of BFA. On the other hand, *ben3* mutants did not show aggregations (Figure 14). Furthermore, *pBEN3::BEN3-GFP* complemented the PIN1 trafficking in *ben3* (*SALK\_024601*). These results indicated that the *BEN3* functions in PIN1 trafficking.

#### **3-2. *BEN3* is involved in PIN1 trafficking from the TGN/EE to the PM**

To investigate whether *BEN3* is involved in PIN1 trafficking from TGN/EE to the PM, I observed the trafficking of newly synthesized PIN1 protein with XVE-PIN1. XVE-PIN1 was introduced into the *ben1-1* and *ben3-1* background. In both genetic backgrounds, induced PIN1 was detectable at the PM within 5 h after estradiol induction (Figure 15A, B). To evaluate the effect of BFA on the delivery of newly synthesized PIN1, BFA was added 2 h after the estradiol treatment and kept for 3 h. In the XVE-PIN1 control line, BFA clearly induced agglomeration of intracellular PIN1 signals and strongly reduced the PM PIN1 localization. However, in the *ben3-1* background, clear PM PIN1 signals were detectable even in the presence of BFA (Figure 15C, D). In the *ben1-1* mutant background, induced PIN1 proteins were often detected from the PM and intracellular compartments under the same conditions (Figure 15C, D). These results show that trafficking of PIN1 from the TGN/EE to the PM is inhibited by BFA and its sensitivity to BFA is affected by *ben1* and *ben3* mutations.

#### **3-4. *SYP4* does not function in the same way as *BEN2***

To investigate the interaction between *BEN2* and other membrane trafficking factors, I tried to reveal the function of SNARE protein *SYP4*. *syp42; syp43* shows the defects of root architecture including short primary root and a lot of lateral roots (Uemura et al. 2012). These phenotypes are similar to that of *ben1; ben2*. I hypothesized that *SYP4* interacts with *BEN2* and contributes to root formation. I established transgenic lines which expressed *SYP43* tissue-specifically in *syp42; syp43* double mutant background.

For this purpose, SYP43 was expressed as GFP fusion protein under the control of either the *PHB*, *SCR* or *PIN2* promoters. Investigation of the GFP signals of the *pPHB::GFP-SYP43*, *pSCR::GFP-SYP43* and *pPIN2::GFP-SYP43* transgenic plants revealed pronounced expression in specific tissues, consistent with other reports (Figure 16A). However, careful inspection of the fluorescent signals in these lines revealed that the GFP signals expanded to the neighboring tissue layers. Unexpectedly all lines of these transgenic lines showed the recovered root architecture (Figure 16B), suggesting that leaky expression and/or intercellular movement of GFP-SYP43 has been sufficient to recover the root growth defects in the *syp42; syp43* double mutants.

#### **4. Response to phosphate starvation**

##### **4-1. *ben1; ben2* is less sensitive to deficiency of phosphate**

The root architecture of *ben1; ben2* which consists of short primary root and a lot of lateral roots is similar to that of seedlings which grow on phosphate starvation medium. To investigate whether the phosphate starvation response happens in *ben1; ben2*, I quantified the root length of seedlings on phosphate starvation media. In Col-0, *ben1*, and *ben2*, the root length was strongly inhibited under the phosphate starvation condition. On the other hand, in *ben1; ben2*, the root elongation was not severely inhibited (Figure 17A, B). This suggests that *ben1; ben2* does not respond to phosphate starvation or that on the normal media, the phosphate starvation response occurs in *ben1; ben2*.

##### **4-2. Iron deposition is enhanced in the root tip of *ben1; ben2* on media including phosphate**

To check whether the phosphate starvation response occurs in *ben1; ben2* on normal media, the iron deposition was observed. As shown in previous reports (Müller et al. 2015), in Col-0, iron was accumulated around QC, and the deposition was enhanced under the conditions of phosphate starvation. Similarly, *ben1* and *ben2* showed the same response. On the other hand, in *ben1; ben2*, the iron deposition around QC and between epidermis and cortex was enhanced on the media including phosphate (Figure 18). This phenotype was recovered with the BEN2 expression under the control of *pBEN2* and *pPHB* but not *pSCR* (Figure 18). This suggests that in *ben1; ben2* phosphate starvation response occurs in the presence of phosphate.

## Discussion

### **The short primary root of *ben1; ben2* is caused by the decrease of cell proliferation which depends on polar transport of auxin**

It has been indicated that BEN1 and BEN2 are involved in membrane trafficking of PIN protein and *ben1; ben2* double mutants exhibit defects in auxin-response gradient (Figure 19) and various developmental processes including growth of primary root (Tanaka et al., 2013). To know whether the developmental defects of *ben1; ben2* is caused by the disruption of PIN polarity and auxin distribution, I investigated the relationship by overexpressing PIN1 which is known to have effect on root growth (Mravec et al., 2008). As reported, the root elongation in Col-0 was inhibited when expression of PIN1 was induced (Figure 2). In contrast, induction of PIN1 expression had only moderate effects on inhibition of root growth in the *ben1; ben2* background. I also checked the relationship between root elongation and auxin biosynthesis with an auxin biosynthesis inhibitor kyn. While kyn strongly inhibited the root growth of Col-0, root growth of *ben1; ben2* was only moderately inhibited (Figure 2). These results indicated that the abnormality of *ben1; ben2* root development might have been caused by the defects of PIN expression or localization, and auxin distribution. In this scenario, defects in PIN localization and reduced auxin accumulation are relevant for the root growth defect, and these might not be further inhibited by PIN1 overexpression and the auxin biosynthesis inhibitor. Thus, my results corroborate the developmental roles of the membrane traffic components BEN1 and BEN2 in regulation of root architecture through PIN polarity and auxin distribution. Curiously, growth of *ben2* single mutant but not that of *ben1* was insensitive to XVE-PIN1, which could be attributed to the different trafficking steps affected by these two mutations (Tanaka et al., 2013) or to the presence of redundant components (Singh et al., 2018).

### **Root formation requires BEN2 expressed in inner tissues**

The clear developmental defects in *ben1; ben2* double mutant as well as PIN1-insensitive *ben2* mutant phenotypes prompted me to further investigate the developmental role of BEN2 by expressing BEN2 under control of various tissue-specific promoters. My results showed that BEN2 regulates PIN trafficking cell-autonomously (Figure 3) and that the tissue-specific expression of BEN2 had differential effects on recovery of *ben1; ben2* root development defects (Figures 4 and 5), allowing us to evaluate the developmental role of BEN2 in specific tissues. Phenotypic studies indicated that root length and lateral root density were consistently recovered when BEN2-GFP was expressed in internal tissues

either by PIN1 or PHB promoters. Based on these results, I concluded that BEN2 expressed in inner tissues mainly regulates root elongation and lateral root formation (Figure 20). In previous studies, it has been suggested that growth of seedling root involves regulators of PIN expression or localization in internal tissues, such as embryonic provascular tissue and vascular tissue of seedling root (Dello Ioio et al., 2008; Wolters et al., 2011). In other report, it was suggested that the density of lateral root is determined by auxin pulse from lateral root cap (Xuan et al., 2016). In my study, BEN2 expression in the inner tissues was relevant for regulation of root growth and lateral root formation. Thus, my results are in good agreement with the crucial roles of internal tissues in supporting PIN-dependent regulation of root growth. Concerning the dense lateral root phenotype of the *ben1; ben2* double mutants, it would be possible that the spread of PIN1 polarity to lateral side of the PM induced auxin leakage to outer tissues, and this might have interfered with auxin pulse.

### **BEN2 expressed in inner tissues affects auxin distribution and cell proliferation**

My findings bring next question how BEN2 in inner tissues regulates root development. To investigate it, I checked the activity of auxin distribution and cell proliferation of transgenic plants. To visualize them, I introduced *DR5rev::Venus-N7* and *CycB1;1-GUS* into the transgenic lines. It has been reported that regulation of PIN expression and cell cycle is of central importance in regulating root meristem size in *Arabidopsis*. As such, alterations of auxin distribution and root meristem sizes often correlate with changes in root growth (Blilou et al., 2005; Dello Ioio et al., 2008; Takahashi et al., 2013). Auxin distribution, as judged by *DR5rev::Venus-N7*, looked to be recovered with BEN2 in inner tissues but not in other tissues (Figure 5C). Transgenic lines which expressed BEN2 in inner tissues showed recovery of cell proliferation zone, too. On the other hand, BEN2 expressed in outer tissues did not contribute to the recovery of meristematic activity (Figure 5B). In this respect, my analysis revealed correlation between enlarged zone of cell division and recovery of root growth. To my surprise, however, *pSCR::BEN2-GFP*, which drove BEN2 expression in endodermis and QC, seemed to moderately expanded the zone of cell division without significantly stimulating root growth (Figure 5). As root length is determined not only by the cell number but also cell length (Rahman et al., 2007; Yang et al., 2017; Ashraf and Rahman, 2019), it is possible that root elongation is also affected in the transgenic lines expressing BEN2 tissue-specifically. Interestingly, exogenously applied auxin or altered growth conditions significantly change the balance between cell proliferation, cell elongation, and root growth (Rahman et al., 2007; Yang et al., 2017). Thus it would be interesting to test whether the tissue-specific BEN2

expression affects any context dependent developmental mechanism for root growth.

In summary, my results suggest that BEN2 has important roles in supporting root growth through PIN-dependent auxin distribution. Using tissue-specific promoters, I showed that BEN2 expressed in inner tissues sufficiently contributes to maintain the auxin distribution and cell proliferation in the root tip. Thus the role of BEN2 in root development can be explained mainly by regulation of tip-ward auxin transport through inner tissues, which affects root elongation and lateral root formation.

### **BEN3/BIG2 is involved in trafficking of PIN1 to the PM**

In this work, I showed that BFA-induced accumulation of PIN1 at the BFA compartment requires BEN3/BIG2 ARF GEF. These results suggest that BEN3/BIG2 is involved in transport of PIN1 to the PM, to the vacuole or both. To gain insight into the trafficking pathway involving BEN3/BIG2, I used conditional expression of PIN1 to evaluate PIN1 trafficking to the PM. Under the experimental conditions, BFA induced PIN1 accumulation at the BFA compartment and inhibited PIN1 delivery to the PM (Figure 15). This BFA effect on the PM targeting was diminished in the *ben3* mutant background, suggesting that BEN3 is involved in endosome to PM trafficking. I speculate that exocytosis-related membranes might be intracellularly sequestered in a BEN3-dependent manner in the presence of BFA. In the absence of BEN3, the sequestering mechanism would be relieved and BFA-resistant ARF GEFs might efficiently deliver PIN1 protein to the PM. Richter et al. (2014) demonstrated that BIG3 ARF GEF is resistant to BFA and is required for trafficking of newly synthesized PIN1-RFP to the PM. Opposite phenotypes of *ben3* and *big3* suits very well with the BFA-resistant nature of BIG3 and sequence-based prediction of BEN3/ BIG2 as being BFA sensitive (Geldner et al. 2003). Taken together, these results provide additional support for the redundant roles of BIG family ARF GEFs in plant development and TGN to PM trafficking in *Arabidopsis*.

### **SYP43 does not functions tissue-specifically in root formation like BEN2**

To gain insights about the interaction between SYP43 and BEN2, I generated transgenic plants expressing SYP43 tissue-specifically. But unexpectedly, tissue-specific expression of SYP43 did not result in the independent response of root formation like BEN2. From this result it was suggested that SYP43 protein could move intercellularly and interacts with not only BEN2 but also other membrane trafficking factors and regulates PIN transport. Since it is known that *Arabidopsis* SYP4 group possesses redundant functions (Uemura et al. 2012). Thus to regulate PIN polarity in response to environmental stimulus in each cell file, BEN2 could be a promising candidate which receives adjustment. But

how BEN2 expression is regulated is not known.

**In *ben1; ben2* phosphate starvation response occurs in the presence of phosphate**

Root architecture is affected by numerous environmental stimuli. To absorb nutrition effectively, some transporters are polarized on the PM. In this research, it was demonstrated that *ben1; ben2* is less sensitive to phosphate starvation. In addition, in *ben1; ben2* on the media including phosphate, iron deposition was enhanced, which is the response to phosphate starvation. From these results I hypothesized that the defects of PIN polarity caused by the mutation in *BEN1* and *BEN2* also affects the signaling involved in phosphate starvation or that the receptor for the concentration of phosphate is overregulated in *ben1; ben2*.

In this thesis, I partially contributed to the elucidation of regulatory mechanisms for root formation by membrane trafficking at TGN/EE.

## Materials and Methods

### Plant Materials and Growth Conditions

Mutants and transgenic marker lines used in this experiment have been described previously: *ben1-1*, *ben2* (Tanaka et al., 2009), pVPS45::VPS45-GFP (Tanaka et al., 2013), *CycB1;1-GUS* (Colón-Carmona et al., 1999). DR5rev::3xVenus-N7 (Heisler et al., 2005) was crossed with Col-0 two times.

Seeds were sterilized in 70% ethanol and rinsed with 100% ethanol. Then they were germinated and grown on 0.4% phytagelsolidified half-concentration Murashige and Skoog (MS) medium supplemented with 1% sucrose (pH 5.9) at 22°C. To prepare the phosphate starvation condition, KH<sub>2</sub>PO<sub>4</sub> was not added in 1/2 MS media.

### Plasmid Construction and Transgenic Plants

To generate pGreen-pPIN1::BEN2-GFP and pGreen-pPHB::BEN2-GFP constructs, a 2.3-kb PIN1 promoter and a 3.0-kb PHB promoter were PCR amplified, and cloned in a GUS-GFP vector (a gift from Yasunori Machida), which was derived from pGreen0029 vector (Hellens et al., 2000), generating pHT035 (pGreen-pPIN1::GUS-GFP) and pHT047 (pGreen-pPHB::GUSGFP). BEN2 coding region including a spacer (AEAAAKEAAKA) was PCR amplified with primers #11459 and #11460, digested with *AscI* and *NcoI*, and cloned into *AscI* and *NcoI* sites of cloning vectors pHT035 and pHT047.

To generate pGreen-pPIN2::BEN2-GFP and pGreen-pSCR::BEN2-GFP constructs, proPIN2 and proSCR fragments were PCR amplified with primers: #9810, #9811, #10968, and #10969, digested with *NotI* and *SallI*, and cloned into *Bsp120I* and *SallI* sites of the pGreen-pPHB::BEN2-GFP, replacing the PHB promoter sequence. To generate transgenic plants, these constructs were transformed into *ben2* and *ben1*; *ben2* by agrobacterium-mediated floral-dip procedure (Clough and Bent, 1998). Transgenic plants were selected on solid media containing 25 mg/L kanamycin.

To generate pMLBarT-pPHB::GFP-SYP43, pMLBarT-pSCR::GFP-SYP43, and pMLBarT-pPIN2::GFP-SYP43 constructs, GFP-SYP43, pPHB, pSCR, and pPIN2 were PCR amplified with primers: #13945, #13946, #10976, #13948, #10968, #13947, #13949, and #13950. GFP-SYP43 was digested with *AscI* and *MluI*, pPHB, pSCR, and pPIN2 were digested with *Bsp120I* and *AscI*, and they were cloned into *BspI* and *MluI* sites of the pBluescript-pGL2-TagRFP-Venus. Each plasmids were digested with *Bsp120I* and *NotI* and cloned into *NotI* site of pMLBarT. To generate transgenic plants, these

constructs were transformed into *syp42*; *syp43* by agrobacterium-mediated floral-dip procedure. Transgenic plants were selected on solid media containing 0.015  $\mu$ l/ml BASTA.

The sequences of the primers are shown below.

#9810 5'-AAGCGGCCGCATCATTACCAGTACCGAATG-3'

#9811 5'-TTGTCTGACTTTGATTTACTTTTTCCGGCGA-3'

#10968 5'-AAAGGGCCCCATGGACATTGGAATCGCCA-3'

#10969 5'-AAAGTCGACGGAGATTGAAGGGTTGTTGGT-3'

#10976 5'-AAAGGGCCCCGAAAATGACACCAACAAG-3'

#11459 5'-AGAGGCGCGCCAACAATGGTTTTGGTTACGTCTGT-3'

#11460 5'-TCACCATGGCCTTAGCAGCAGCCTCCTTAGCAGCAGCCTCAGCCA-  
CCATATGGCTACCTGA-3'

#13945 5'-AAAGGCGCGCCTGAAACAATGGTGAGCAAGGGCGA-3'

#13946 5'-TTTACGCGTTCACAACAGAATCTCCTTGA-3'

#13947 5'-AAAGGCGCGCCGGAGATTGAAGGGTTGTTGGT-3'

#13948 5'-AAAGGCGCGCCAGCTCAAAGTCAGAAATAAGGAA-3'

#13949 5'-AAAGGGCCCATCATTACCAGTACCGAATG-3'

#13950 5'-AAAGGCGCGCCTTTGATTTACTTTTTCCGG-3'

### **Drug Treatment**

BFA (Molecular Probes, B7450) and L-Kynurenine (Kyn, Tokyo Chemical Industry, K0016) was diluted with liquid Arabidopsis medium from 50 mM stock solution in DMSO. For cell wall staining, seedlings were immersed in 4% (w/v) paraformaldehyde in PBS buffer, supplemented with SR2200 (1:500; Renaissance Chemicals), incubated under vacuum for 1h, rinsed with PBS, and mounted with ClearSee solution (Kurihara et al., 2015). For live cell imaging, seedlings were mounted in 1/2 MS medium.

### **Immunolocalization and Microscopy**

Immunolocalization was performed as described (Kitakura et al., 2017). Briefly, seedlings were fixed with 4% paraformaldehyde in PBS (1h), adhered on MAS-coat slides (Matsunami glass, S9441), permeabilized by sequential treatment with 2.5% to 3.0% driselase (30 min at 37°C) and a mixture of 10% DMSO and 1%NP-40 substitute (1 h). 3%BSA in PBS was used for blocking and dilution of antibodies as follows: goat anti-PIN1 (1:400; Santa Cruz, sc-27163), rabbit anti-PIN2 (1:2000) (Abas et al., 2006), Cy3-conjugated secondary anti-rabbit (1:600; Sigma, C2306) and DyLight 649-conjugated

secondary anti-goat (1:400; Jackson Immuno Research, 705-495-147) antibodies. After incubation with the antibody solutions, samples were washed with PBS and mounted in ClearSee solution (Kurihara et al., 2015). Confocal laser-scanning microscopy was performed with a Carl Zeiss LSM710 microscope.

### **Root Phenotypic Analysis**

For analysis of meristem size, seedlings were fixed and stained with SR2200 (1:500), diluted in a fixative solution (4% paraformaldehyde, 0.05% Triton X100 in PBS buffer). Samples were then mounted with ClearSee solution. At least three biological replicates were performed and similar results were obtained. Quantitative evaluation was performed with ImageJ. Meristem size was defined as distance between QC and cortex cell which expanded rapidly. To evaluate the distribution of CycB1;1-GUS positive cells in the root tips, distance along longitudinal axis from QC to each cell with strong GUS positive signal was measured by using ImageJ. At least 30 cells from 3 to 10 seedlings from each genotype were scored in one experiment. Two independent experiments gave essentially the same results.

### **GUS Staining**

For detection of GUS activity, seedlings were rinsed in a preincubation buffer [0.1M sodium phosphate buffer (pH 7.0); 2 mM potassium ferrocyanide; 2mM potassium ferricyanide]. The buffer was then substituted with a GUS-staining buffer supplemented with 0.25 mg/mL 5-Bromo-4-chloro-3-indolyl b-D-glucuronide (xgluc.) (Rose Scientific, ES-1007-001) and incubated at 37°C in the darkness. After coloration, GUS staining buffer was substituted by 70% ethanol. Seedlings were hydrated and finally soaked in ClearSee solution.

### **Perls Staining**

For detection of iron deposition, seedlings were stained with Perls staining (Müller et al. 2015). Seedlings were incubated in staining buffer with 1.4% (v/v) HCl, 4% (w/v) K-ferrocyanide at room temperature for 30 min. The staining buffer was substituted by water. Finally seedlings were mounted with chloral hydrate.

### **Statistical Analysis**

Statistical analyses were performed by using Excel 2016 (Microsoft), PRISM 5 (GraphPad) software, or R version 4.0.2. I designated significant difference as  $0.01 < p\text{-value} \leq 0.05$  (\*) and  $p\text{-value} \leq 0.01$  (\*\*). Students' t-tests were performed to compare

the outcomes between paired comparison groups which determined by the mutants, separately. In the case that there are multiple pair-wise combinations within a single hypothesis testing process, we checked whether at least two group means are different or not using one-way ANOVA (analysis of variance) before specific paired groups comparison. When the result of the overall test is significant, the paired comparison using Students' t-test was intended for specific paired groups of interest, which have been planned *a priori*.

In these analyses, we did not adjust the significance level for multiple comparisons, because Rosner (2010, 534) suggested that if the comparison groups are relatively few and the specific pairs are selected planned in advance, and these pair-wise analyses are conducted only when one-way ANOVA test is statistically significant, the multiple-comparisons issue does not occur.

Furthermore, we estimated the effect of the treatment on the outcomes among each mutant group using Students' t-tests. Moreover, in order to examine whether the treatment effect is modified by the mutants, we performed two-way ANOVA.

All statistical hypothesis tests were performed with two-sided 5% significance level.

## **Acknowledgement**

I thank Jiri Friml, Peter Doerner, Christian Luschnig, Roger Hellens, Tomohiro Uemura, Elliot M. Meyerowitz and Hidehiro Fukaki for generously providing published materials. I thank Yasunori Machida for the gift of the plasmid vector. I thank Kayoko Kawamura for her technical assistance in transformation and genotyping. I thank Prof. Tatsuo Kakimoto, Dr. Shinobu Takatda, and the current and former members of Kakimoto lab for their helpful discussion and support. This work was supervised by Dr. Hirokazu Tanaka, I especially express my deepest gratitude to him. Finally, I deeply thank my husband, Daijiro Kabata, and our daughter, Iku Kabata, for their support.

## References

- Abas, L., Benjamins, R., Malenica, N., Paciorek, T., Wiśniewska, J., Moulinier-Anzola, J. C., et al. (2006). Intracellular trafficking and proteolysis of the Arabidopsis auxin-efflux facilitator PIN2 are involved in root gravitropism. *Nat. Cell Biol.* 8, 249–256. doi: 10.1038/ncb1369
- Ashraf, M. A., and Rahman, A. (2019). Cold stress response in Arabidopsis thaliana is mediated by GNOM ARF-GEF. *Plant J.* 97, 500–516. doi: 10.1111/tpj.14137
- Banda, J., Bellande, K., von Wangenheim, D., Goh, T., Guyomarc'h, S., Laplaze, L., et al. (2019). Lateral Root Formation in Arabidopsis: A Well-Ordered LRExit. *Trends Plant Sci.* 24, 826–839. doi: 10.1016/j.tplants.2019.06.015
- Blilou, I., Xu, J., Wildwater, M., Willemsen, V., Paponov, I., Frimi, J., et al. (2005). The PIN auxin efflux facilitator network controls growth and patterning in Arabidopsis roots. *Nature* 433, 39–44. doi: 10.1038/nature03184
- Casanova-Sáez, R., and Voß, U. (2019). Auxin Metabolism Controls Developmental Decisions in Land Plants. *Trends Plant Sci.* 24, 741–754. doi: 10.1016/j.tplants.2019.05.006
- Clough, S. J., and Bent, A. F. (1998). Floral dip: A simplified method for Agrobacterium-mediated transformation of Arabidopsis thaliana. *Plant J.* 16, 735–743. doi: 10.1046/j.1365-313x.1998.00343.x
- Colón-Carmona, A., You, R., Haimovitch-Gal, T., and Doerner, P. (1999). Spatiotemporal analysis of mitotic activity with a labile cyclin-GUS fusion protein. *Plant J.* 20, 503–508. doi: 10.1046/j.1365-313x.1999.00620.x
- Dello Ioio, R., Nakamura, K., Moubayidin, L., Perilli, S., Taniguchi, M., Morita, M. T., et al. (2008). A genetic framework for the control of cell division and differentiation in the root meristem. *Science* 322, 1380–1384. doi: 10.1126/science.1164147
- Ericsson, T. (1995) Growth and shoot: root ratio of seedlings in relation to nutrient availability. *Plant Soil* 168, 205–214 (1995). doi: 10.1007/BF00029330

- Friml, J., Vieten, A., Sauer, M., Weijers, D., Schwarz, H., Hamann, T., et al. (2003). Efflux-dependent auxin gradients establish the apical-basal axis of Arabidopsis. *Nature* 426, 147–153. doi: 10.1038/nature02085
- Fukaki H, Tameda S, Masuda H, Tasaka M. Lateral root formation is blocked by a gain-of-function mutation in the SOLITARY-ROOT/IAA14 gene of Arabidopsis. *Plant J.* 2002 Jan;29(2):153-68. doi: 10.1046/j.0960-7412.2001.01201.x.
- Geldner, N., Anders, N., Wolters, H., Keicher, J., Kornberger, W., Müller, P., et al. (2003). The Arabidopsis GNOM ARF-GEF mediates endosomal recycling, auxin transport, and auxin-dependent plant growth. *Cell* 112, 219–230. doi: 10.1016/S0092-8674(03)00003-5
- Grunewald, W., and Friml, J. (2010). The march of the PINs: developmental plasticity by dynamic polar targeting in plant cells. *EMBO J.* 29, 2700–2714. doi: 10.1038/emboj.2010.181
- Heisler, M. G., Ohno, C., Das, P., Sieber, P., Reddy, G. V., Long, J. A., et al. (2005). Patterns of auxin transport and gene expression during primordium development revealed by live imaging of the Arabidopsis inflorescence meristem. *Curr. Biol.* 15, 1899–1911. doi: 10.1016/j.cub.2005.09.052
- Hellens, R. P., Anne Edwards, E., Leyland, N. R., Bean, S., and Mullineaux, P. M. (2000). pGreen: A versatile and flexible binary Ti vector for Agrobacterium mediated plant transformation. *Plant Mol. Biol.* 42, 819–832. doi: 10.1023/A:1006496308160
- Huang, F., Zago, M. K., Abas, L., Marion, A., Van, Galván-ampudia, C. S., van Marion, A., et al. (2010). Phosphorylation of conserved PIN motifs directs Arabidopsis PIN1 polarity and auxin transport. *Plant Cell* 22, 1129–1142. doi: 10.1105/tpc.109.072678
- Kitakura, S., Adamowski, M., Matsuura, Y., Santuari, L., Kouno, H., Arima, K., et al. (2017). BEN3/BIG2 ARF GEF is involved in brefeldin a-sensitive trafficking at the trans-golgi network/early endosome in arabidopsis thaliana. *Plant Cell Physiol.* 58, 1801–1811. doi: 10.1093/pcp/pcx118

- Kleine-Vehn, J., Dhonukshe, P., Sauer, M., Brewer, P. B., Wiśniewska, J., Paciorek, T., et al. (2008). ARF GEF-Dependent Transcytosis and Polar Delivery of PIN Auxin Carriers in Arabidopsis. *Curr. Biol.* 18, 526–531. doi: 10.1016/j.cub.2008.03.021
- Kurihara, D., Mizuta, Y., Sato, Y., and Higashiyama, T. (2015). ClearSee: a rapid optical clearing reagent for whole-plant fluorescence imaging. *Development* 142, 4168–4179. doi: 10.1242/dev.127613
- Ljung, K., Hull, A. K., Celenza, J., Yamada, M., Estelle, M., Normanly, J., et al. (2005). Sites and regulation of auxin biosynthesis in arabidopsis roots. *Plant Cell* 17, 1090–1104. doi: 10.1105/tpc.104.029272
- Miyashima, S., Koi, S., Hashimoto, T., and Nakajima, K. (2011). Non-cell-autonomous microRNA 165 acts in a dose-dependent manner to regulate multiple differentiation status in the Arabidopsis root. *Development* 138, 2303–2313. doi: 10.1242/dev.060491
- Mockaitis, K., and Estelle, M. (2008). Auxin receptors and plant development: a new signaling paradigm. *Annu. Rev. Cell Dev. Biol.* 24, 55–80. doi: 10.1146/annurev.cellbio.23.090506.123214
- Mravec, J., Kubeš, M., Bielach, A., Gaykova, V., Petrášek, J., Skůpa, P., et al. (2008). Interaction of PIN and PGP transport mechanisms in auxin distribution dependent development. *Development* 135, 3345–3354. doi: 10.1242/dev.021071
- Müller J, Toev T, Heisters M, Teller J, Moore KL, Hause G, Dinesh DC, Bürstenbinder K, Abel S. Iron-dependent callose deposition adjusts root meristem maintenance to phosphate availability. *Dev Cell.* 2015 Apr 20;33(2):216-30. doi: 10.1016/j.devcel.2015.02.007.
- Naramoto, S., Otegui, M. S., Kutsuna, N., de Rycke, R., Dainobu, T., Karampelias, M., et al. (2014). Insights into the localization and function of the membrane trafficking regulator GNOM ARF-GEF at the Golgi apparatus in Arabidopsis. *Plant Cell* 26, 3062–3076. doi: 10.1105/tpc.114.125880
- Péret B, Clément M, Nussaume L, Desnos T. Root developmental adaptation to phosphate starvation: better safe than sorry. *Trends Plant Sci.* 2011 Aug;16(8):442-50. doi:

10.1016/j.tplants.2011.05.006.

Perilli S, Di Mambro R, Sabatini S. Growth and development of the root apical meristem. *Curr Opin Plant Biol.* 2012 Feb;15(1):17-23. doi: 10.1016/j.pbi.2011.10.006.

Petricka, J. J., Winter, C. M., and Benfey, P. N. (2012). Control of Arabidopsis Root Development. *Annu. Rev. Plant Biol.* 63, 563–590. doi: 10.1146/annurevplant-042811-105501

Rahman, A., Bannigan, A., Sulaman, W., Pechter, P., Blancaflor, E. B., and Baskin, T. (2007). Auxin, actin and growth of the Arabidopsis thaliana primary root. *Plant J.* 50, 514–528. doi: 10.1111/j.1365-313X.2007.03068.x

Rosner , B. (2010) Fundamentals of Biostatistics, 7<sup>th</sup> edition. Cengage Learning, Inc.

Sauer, M., and Kleine-Vehn, J. (2019). PIN-FORMED and PIN-LIKES auxin transport facilitators. *Development* 146, dev168088. doi: 10.1242/dev.168088

Sebastian, J., Ryu, K. H., Zhou, J., Tarkowská, D., Tarkowski, P., Cho, Y. H., et al. (2015). PHABULOSA Controls the Quiescent Center-Independent Root Meristem Activities in Arabidopsis thaliana. *PloS Genet.* 11, 1–27. doi: 10.1371/journal.pgen.1004973

Singh, M. K., Richter, S., Beckmann, H., Kientz, M., Stierhof, Y. D., Anders, N., et al. (2018). A single class of ARF GTPase activated by several pathway-specific ARFGEFs regulates essential membrane traffic in Arabidopsis. *PloS Genet.* 14, e1007795. doi: 10.1371/journal.pgen.1007795

Sugawara, S., Mashiguchi, K., Tanaka, K., Hishiyama, S., Sakai, T., Hanada, K., et al. (2015). Distinct Characteristics of Indole-3-Acetic Acid and Phenylacetic Acid, Two Common Auxins in Plants. *Plant Cell Physiol.* 56, 1641–1654. doi: 10.1093/pcp/pcv088

Takahashi, N., Kajihara, T., Okamura, C., Kim, Y., Katagiri, Y., Okushima, Y., et al. (2013). Cytokinins control endocycle onset by promoting the expression of an APC/C activator in arabidopsis roots. *Curr. Biol.* 23, 1812–1817. doi: 10.1016/.cub.2013.07.051

Tanaka, H., Dhonukshe, P., Brewer, P. B., and Friml, J. (2006). Spatiotemporal

asymmetric auxin distribution: A means to coordinate plant development. *Cell Mol. Life Sci.* 63, 2738–2754. doi: 10.1007/s00018-006-6116-5

Tanaka, H., Kitakura, S., De Rycke, R., De Groodt, R., and Friml, J. (2009). Fluorescence Imaging-Based Screen Identifies ARF GEF Component of Early Endosomal Trafficking. *Curr. Biol.* 19, 391–397. doi: 10.1016/j.cub.2009.01.057

Tanaka, H., Kitakura, S., Rakusová, H., Uemura, T., Feraru, M. I., de Rycke, R., et al. (2013). Cell Polarity and Patterning by PIN Trafficking through Early Endosomal Compartments in *Arabidopsis thaliana*. *PloS Genet.* 9, e1003540. doi: 10.1371/journal.pgen.1003540

Tanaka, H., Nodzynski, T., Kitakura, S., Feraru, M. I., Sasabe, M., Ishikawa, T., et al. (2014). BEX1/ARF1A1C is required for BFA-sensitive recycling of PIN auxin transporters and auxin-mediated development in *Arabidopsis*. *Plant Cell Physiol.* 55, 737–749. doi: 10.1093/pcp/pct196

Uemura T, Kim H, Saito C, Ebine K, Ueda T, Schulze-Lefert P, Nakano A. Qa-SNAREs localized to the trans-Golgi network regulate multiple transport pathways and extracellular disease resistance in plants. *Proc Natl Acad Sci U S A.* 2012 Jan 31;109(5):1784-9. doi: 10.1073/pnas.1115146109.

Vanneste, S., and Friml, J. (2009). Auxin: A Trigger for Change in Plant Development. *Cell* 136, 1005–1016. doi: 10.1016/j.cell.2009.03.001

Vieten, A., Vanneste, S., Wiśniewska, J., Benková, E., Benjamins, R., Beeckman, T., et al. (2005). Functional redundancy of PIN proteins is accompanied by auxin dependent cross-regulation of PIN expression. *Development* 132, 4521–4531. doi: 10.1242/dev.02027

Wiśniewska, J., Xu, J., Seifertová, D., Brewer, P. B., Ružička, K., Blilou, I., et al. (2006). Polar PIN Localization Directs Auxin Flow in Plants. *Science* 312, 883. doi: 10.1126/science.1121356

Wolters, H., Anders, N., Geldner, N., Gavidia, R., and Jürgens, G. (2011). Coordination of apical and basal embryo development revealed by tissue specific GNOM functions.

Development 138, 117–126. doi: 10.1242/dev.059147

Xuan, W., Band, L. R., Kumpf, R. P., Van Damme, D., Parizot, B., De Rop, G., et al. (2016). Cyclic programmed cell death stimulates hormone signaling and root development in *Arabidopsis*. *Science* 351, 384–387. doi: 10.1126/science.aad2776

Yang, X., Dong, G., Palaniappan, K., Mi, G., and Baskin, T. I. (2017). Temperature compensated cell production rate and elongation zone length in the root of *Arabidopsis thaliana*. *Plant Cell Environ.* 40, 264–276. doi: 10.1111/pce.12855

Zhang, X., Adamowski, M., Marhava, P., Tan, S., Zhang, Y., Rodriguez, L., et al. (2020). *Arabidopsis* Flippases Cooperate with ARF GTPase Exchange Factors to Regulate the Trafficking and Polarity of PIN Auxin Transporters. *Plant Cell* 32, 1644–1664. doi: 10.1105/tpc.19.00869

Zwiewka, M., Bilanovičová, V., Seifu, Y. W., and Nodzyński, T. (2019). The Nuts and Bolts of PIN Auxin Efflux Carriers. *Front. Plant Sci.* 10, 985. doi: 10.3389/fpls.2019.00985

## Figures

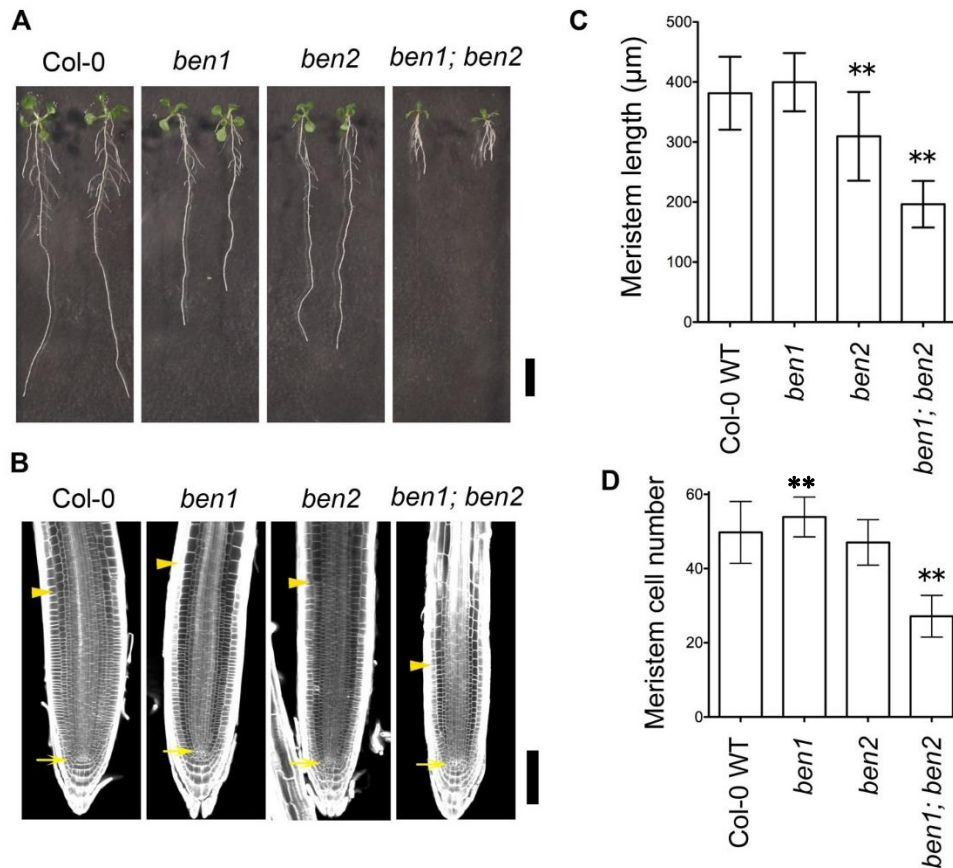


### Figure 1. Phenotype of *ben1; ben2* mutant roots.

(A) Gross morphology of wildtype Col-0, *ben1*, *ben2*, and *ben1; ben2* mutants at 10 days after germination (DAG). (B–D) Meristem size of primary roots in Col-0, *ben1*, *ben2*, and *ben1; ben2* at 5 DAG. The arrows and arrowheads in (B) indicate the positions of the QC and the boundary between the meristematic zone and the elongation zone of root, respectively. Representative data from at least three independent biological replications are shown. Asterisks (\*\*) in the graphs (C, D) represent significant difference ( $p$ -value  $\leq 0.01$  by Student's *t*-test). Error bars represent SD ( $n \geq 15$  for (C) and  $n \geq 19$  for (D)). Scale bars: 10 mm in (A); 100  $\mu\text{m}$  in (B).

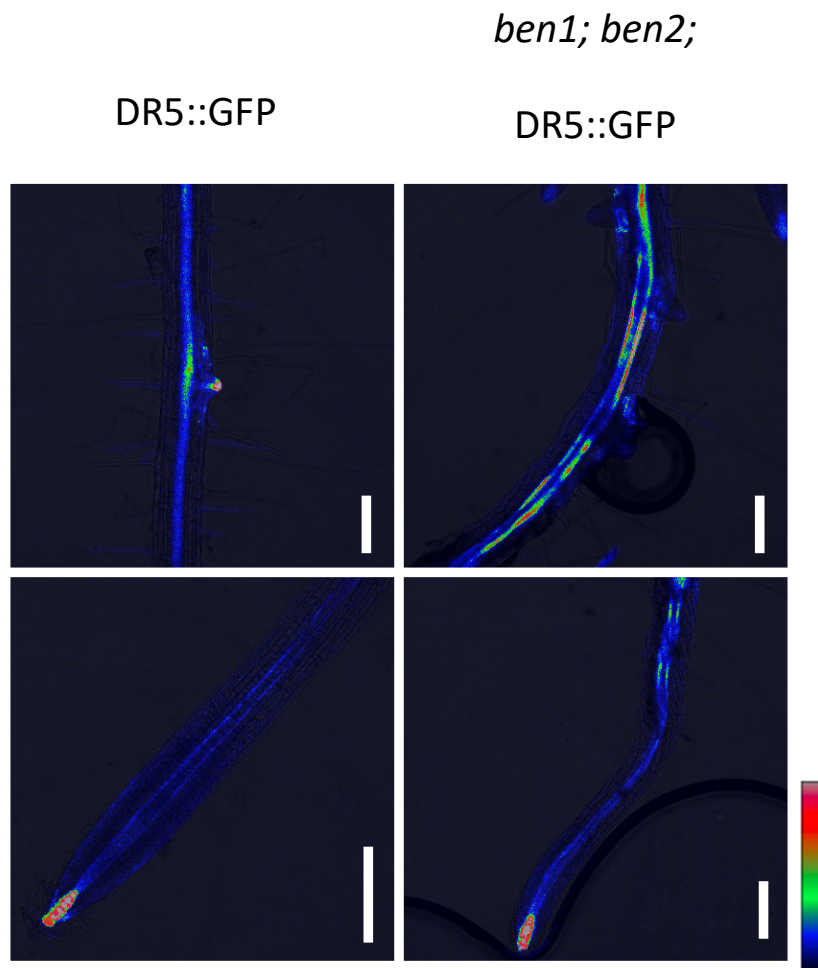


**Figure 2. DR5::GFP distribution in Col-0 and *ben1; ben2*.**

The distribution of DR5::GFP in wildtype Col-0 and *ben1; ben2* mutants at 9 days after germination (DAG). Representative data from at least three independent biological replications are shown. Scale bars: 200  $\mu$ m.

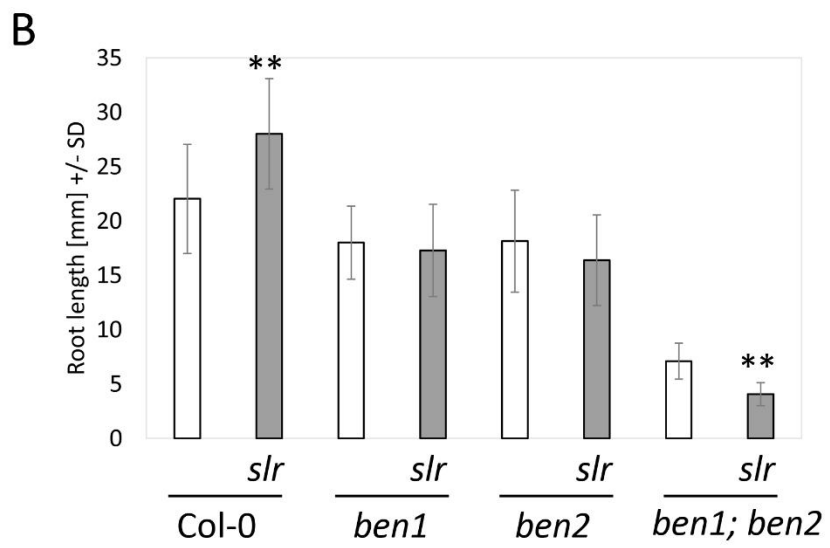
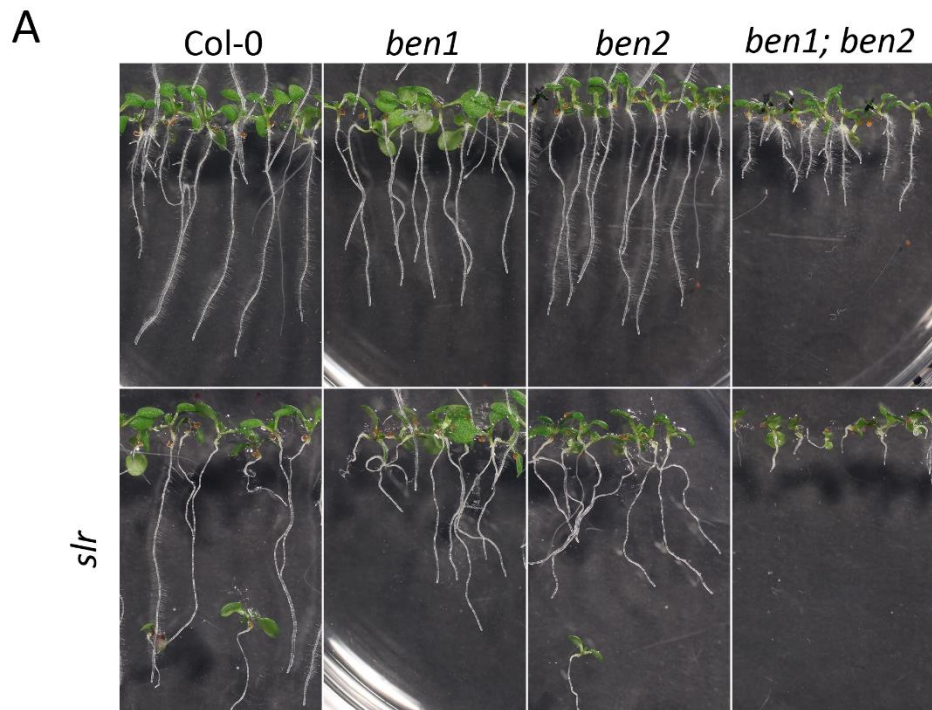


**Figure 3. Alteration of root elongation by inhibiting of lateral root formation.**

(A, B) Morphology of seedlings (A) and root length (B) of Col-0, *ben1*, *ben2*, *ben1; ben2*, *slr/+*, *ben1; slr/+*, *ben2; slr*, and *ben1; ben2; slr/+* at 7 DAG. (B) With respect to *slr/+*, the only seedlings which did not have lateral root was quantified. Error bars represent SD [47 ≥ n ≥ 12]. Representative results from at least two biological replicates were shown. Asterisks indicate significant difference as compared with corresponding control experiments [0.01 < p-value ≤ 0.05 (\*) and p-value ≤ 0.01 (\*\*)]. Scale bar: 10 mm.

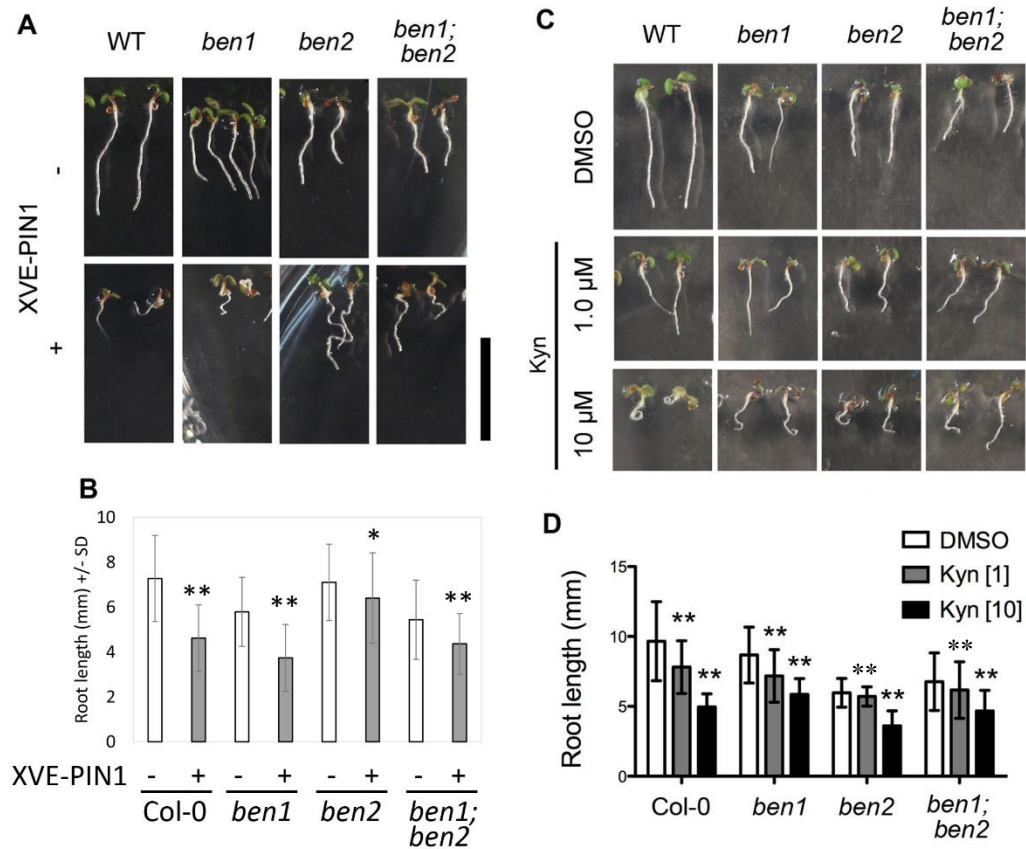


**Figure 4. Inhibition of root elongation by compromised auxin transport and biosynthesis.**

(A, B) Morphology of seedlings (A) and root length (B) of Col-0, *ben1*, *ben2*, and *ben1; ben2* with or without XVE-PIN1 grown in the presence of estradiol (4 μM) at 5 DAG. (C, D) Gross morphology of seedlings (C) and root length (D) of Col-0, *ben1*, *ben2*, and *ben1; ben2* at 5 DAG with treatment of DMSO and Kyn (1.0 μM, and 10 μM). Error bars in (B, D) represent SD [n ≥ 51 for (B); n ≥ 13 for (D)]. Representative results from at least two biological replicates were shown. Asterisks indicate significant difference as compared with corresponding control experiments [0.01 < p-value ≤ 0.05 (\*) and p-value ≤ 0.01 (\*\*)]. The treatment effects were different between the mutants with statistical significance, which was assessed using two-way ANOVA. Scale bars: 10 mm in (A, C).

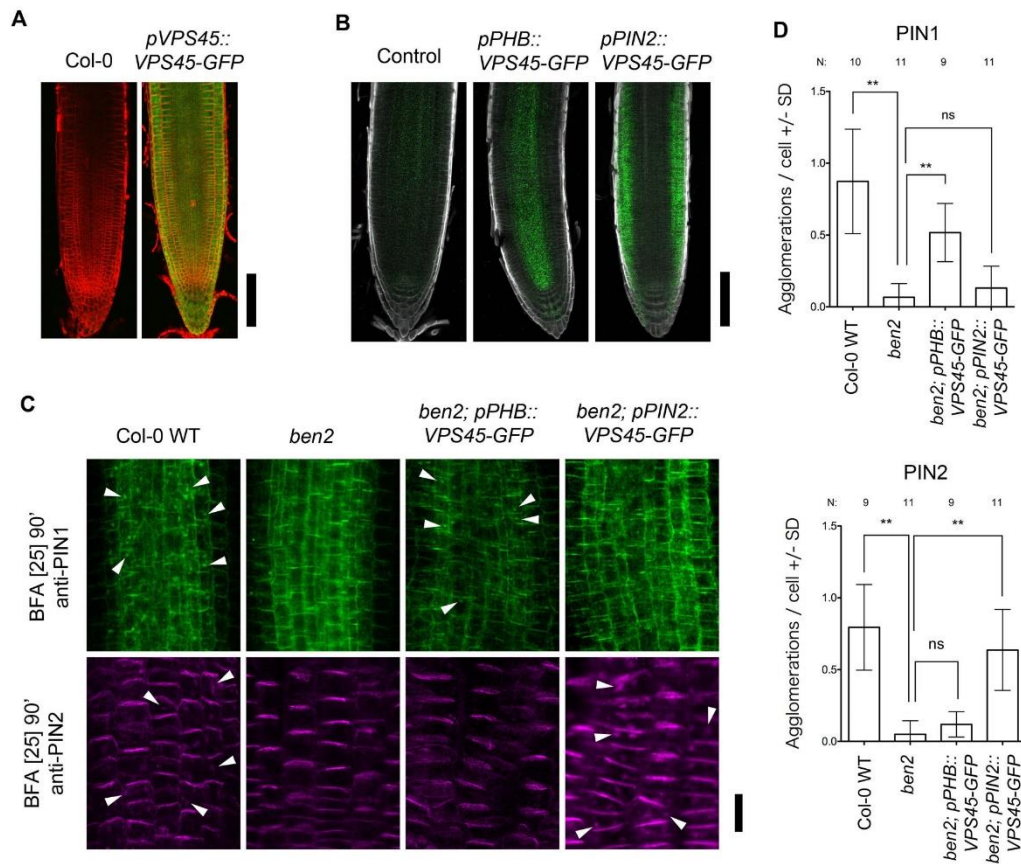


**Figure 5. BEN2/VPS45 regulates PIN trafficking cell-autonomously.**

(A) Root tips of Col-0 and *pVPS45::VPS45-GFP* at 7 DAG. (B) Root tips of *ben2* single mutant (control) and *ben2* mutants harboring *pPHB::VPS45-GFP* and *pPIN2::VPS45-GFP* constructs at 7 DAG. (C) Immunolocalization of PIN1 and PIN2 in BFA treated Col-0, *ben2*, *ben2; pPHB::VPS45-GFP*, and *ben2; pPIN2::VPS45-GFP* seedlings. PIN1 localization in vasculature (green signals in upper panels) and PIN2 in epidermis (magenta signals in lower panels) are indicated. Arrowheads indicate agglomeration of PIN proteins. Representative images from at least three independent experiments are shown. (D) Quantification of PIN1 and PIN2 agglomeration in the BFA-treated seedling roots. Number of agglomeration (>1  $\mu\text{m}^2$  in cross section) per cell was scored in at least 10 cells in each root. Data from 9 to 11 seedling root (187–378 cells) from each genotype were evaluated. Asterisks (\*\*) represent significant difference (p-value  $\leq 0.01$  by Student's t-test). Scale bars: 100  $\mu\text{m}$  in (A, B) and 20  $\mu\text{m}$  in (C).

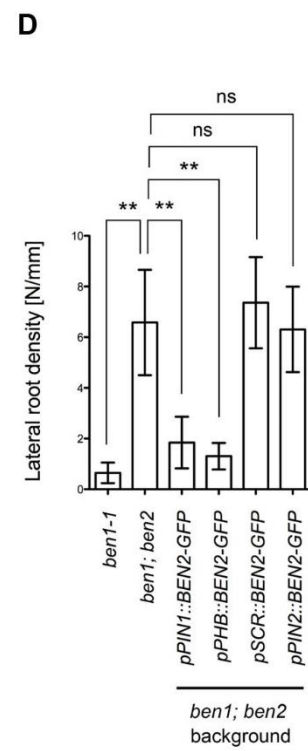
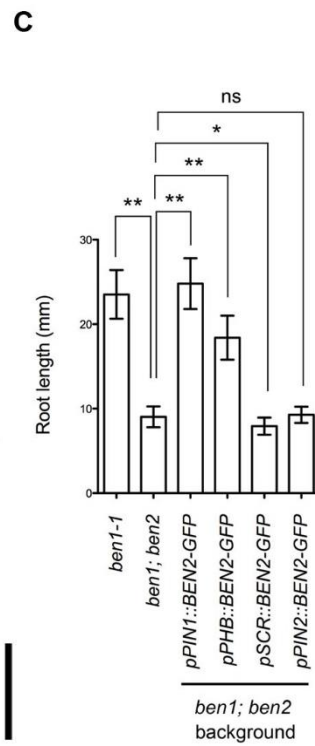
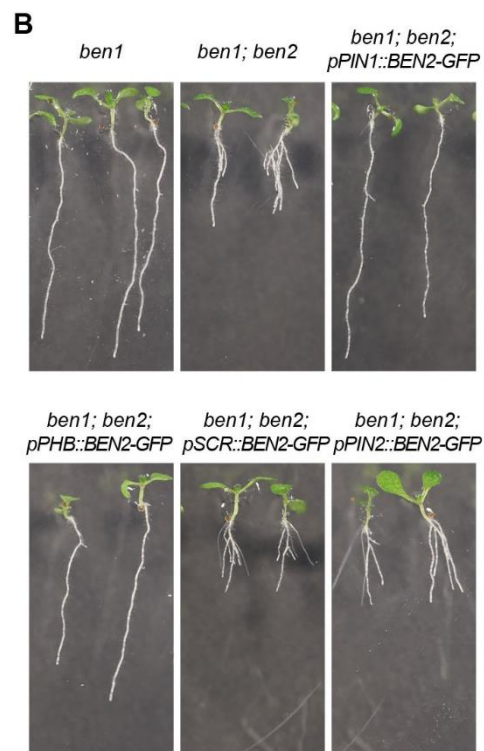
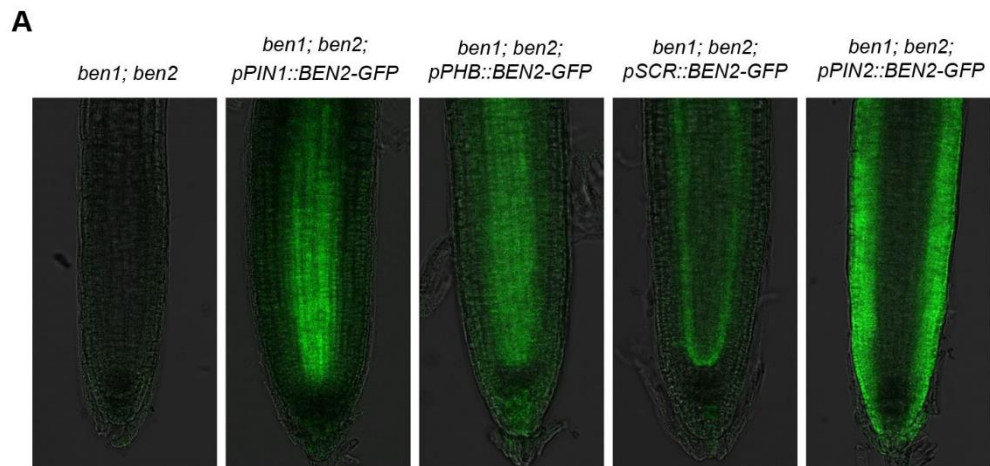


**Figure 6. Phenotypes of transgenic plants expressing *BEN2/VPS45-GFP* under control of tissue-specific promoters.**

(A) Expression of *BEN2/VPS45-GFP* on the *ben1; ben2* double mutant background. Whereas *BEN2/VPS45-GFP* expressed under *PIN1* and *PHB* promoters were mainly detected in stele, GFP was detected mainly in QC and endodermis in *pSCR::BEN2/VPS45-GFP* and in the outer tissues in *pPIN2::BEN2/VPS45-GFP* lines. Note that *ben1; ben2* double mutant which does not harbor GFP has faint autofluorescence. (B) Seedlings of mutants and transgenic lines at 7 DAG. (C-E) Root length (C), number of lateral root per root (D), and lateral root density (E) of mutants and transgenic lines at 7 DAG. At least three independent experiments resulted in similar results. Error bars indicate SD ( $n \geq 14$ ). Results of statistic evaluation by Mann-Whitney U-test was shown as follows:  $0.01 < p\text{-value} \leq 0.05$  (\*);  $p\text{-value} \leq 0.01$  (\*\*) and not significant (ns). Scale bars: 100  $\mu\text{m}$  in (A) and 10 mm in (B).

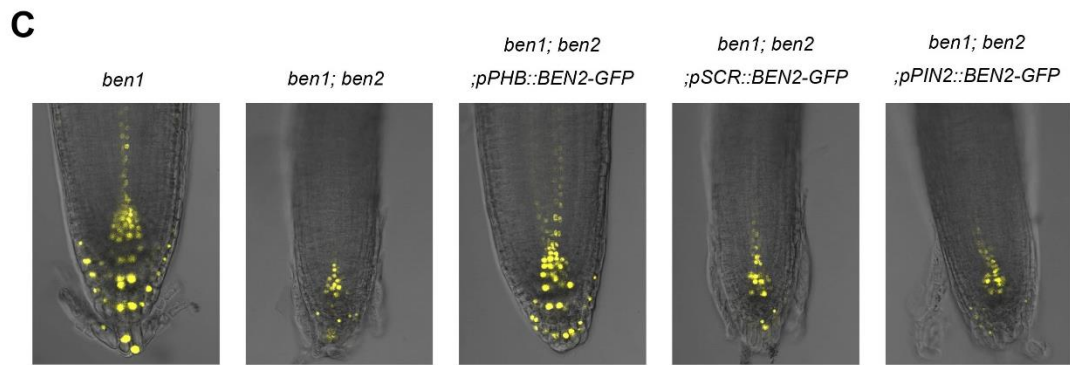
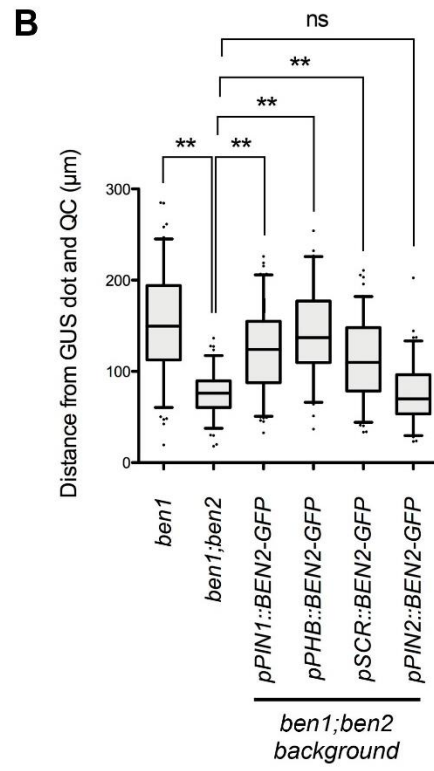
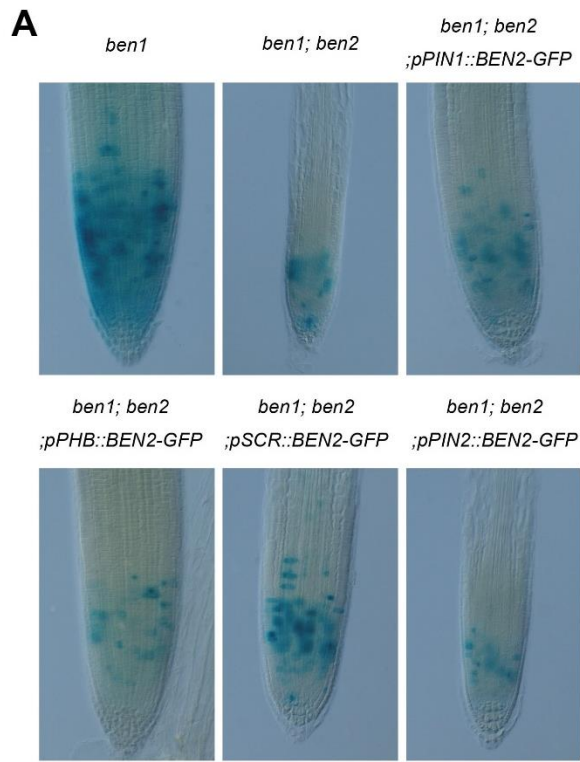


**Figure 7. Expression patterns of *CycB1;1-GUS* and *DR5rev::Venus-N7* in transgenic lines expressing *BEN2/VPS45-GFP* driven by tissue-specific promoters.**

(A) Root tips of mutants and the transgenic lines expressing *CycB1;1-GUS* at 7 DAG. Three independent experiments resulted in similar results. (B) Distribution patterns of cells with strong *CycB1;1-GUS* activity in mutants and transgenic lines expressing *BEN2/VPS45-GFP*, shown as distance from QC at 7 DAG. Location of each GUS-positive cell was measured and presented as boxes (25–75 percentile) and whiskers (5–95 percentile). The dots represent outliers. The graph represents the data from the independent experiments ( $n \geq 73$ ). Results of statistic evaluation was shown as follows:  $0.01 < p\text{-value} \leq 0.05$  (\*);  $p\text{-value} \leq 0.01$  (\*\*) and not significant (ns). (C) Auxin response distribution in root tips of *ben1* and *ben1; ben2* mutants, and *ben1; ben2* double mutants harboring *BEN2/VPS45-GFP* constructs, as visualized by *DR5rev::Venus-N7* at 7 DAG. Scale bars: 100  $\mu\text{m}$  in (A) and 50  $\mu\text{m}$  in (C).

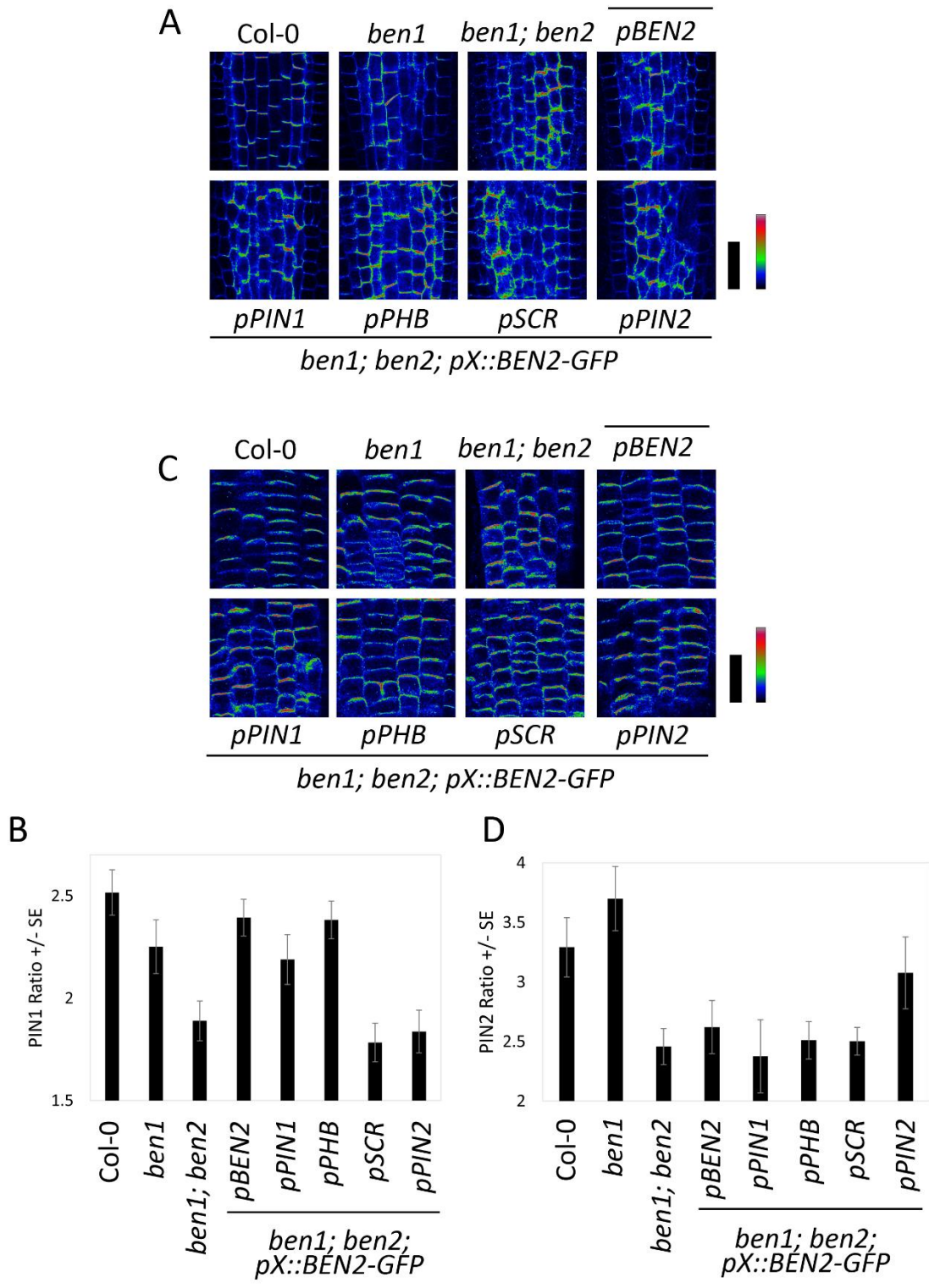


**Figure 8. PIN1 and PIN2 polarity in transgenic lines expressing *BEN2/VPS45-GFP* driven by tissue-specific promoters.**

(A, C) Immunolocalization of PIN1 (A) and PIN2 (B) in Col-0, *ben1*, *ben1; ben2*, *ben1; ben2; pBEN2::BEN2-GFP*, *ben1; ben2; pPIN1::BEN2-GFP*, *ben1; ben2; pPHB::BEN2-GFP*, *ben1; ben2; pSCR::BEN2-GFP*, and *ben1; ben2; pPIN2::BEN2-GFP* seedlings at 4 DAG. PIN1 localization in vasculature and PIN2 in epidermis are indicated. (B, D) Quantification of PIN1 (B) and PIN2 (D) polarity in each seedling roots. In PIN1, the intensity of GFP fluorescence at basal side was divided by that at the lateral side. And in PIN2, that at the apical side was divided by that at the lateral side. In each seedling, 5 cells were calculated. At least two independent experiments resulted in similar results. Error bars indicate SE ( $n \geq 25$  for (B);  $n \geq 15$  for (D)). Color codes indicate the intensity of fluorescence. Scale bars: 20  $\mu\text{m}$  in (A, C).

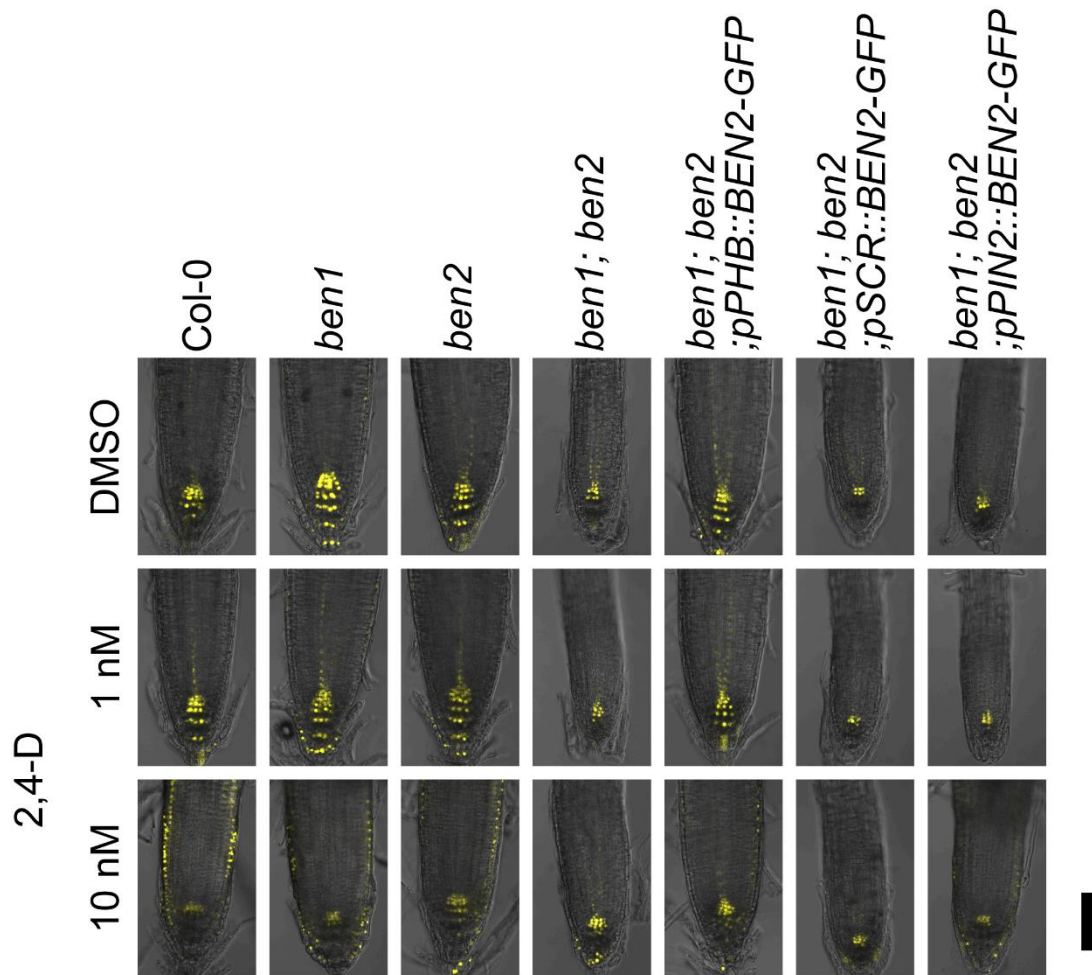


**Figure 9. Expression patterns of *DR5rev::3xVenus-N7* in transgenic lines expressing *BEN2/VPS45-GFP* driven by tissue-specific promoters treated with 2,4-D.**

Expression patterns of *DR5rev::3xVenus-N7* in *DR5rev::3xVenus-N7*, *ben1; DR5rev::3xVenus-N7*, *ben2; DR5rev::3xVenus-N7*, *ben1; ben2; DR5rev::3xVenus-N7*, *ben1; ben2; pPIN1::BEN2-GFP*; *DR5rev::3xVenus-N7*, *ben1; ben2; pPHB::BEN2-GFP*; *DR5rev::3xVenus-N7*, *ben1; ben2; pSCR::BEN2-GFP*; *DR5rev::3xVenus-N7*, and *ben1; ben2; pPIN2::BEN2-GFP*; *DR5rev::3xVenus-N7* seedlings at 7 DAG. Seedlings were treated with DMSO (upper images), 1 nM 2,4-D (middle images), and 10 nM 2,4-D (lower images). Scale bar: 100  $\mu$ m.

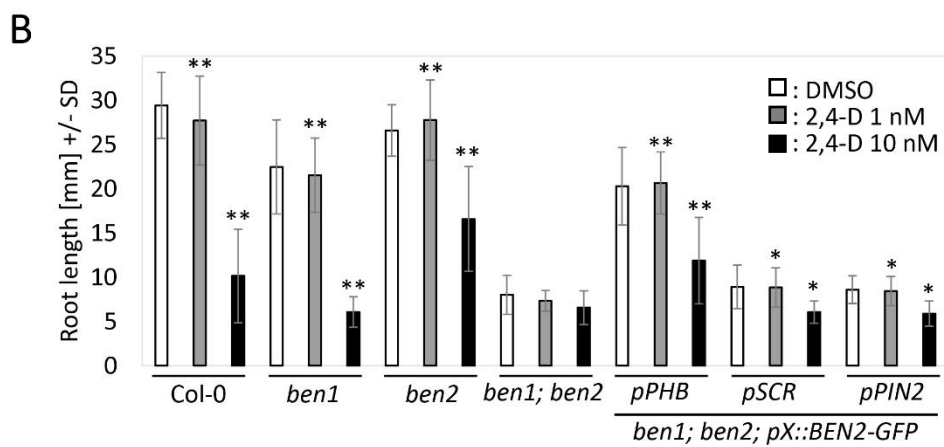
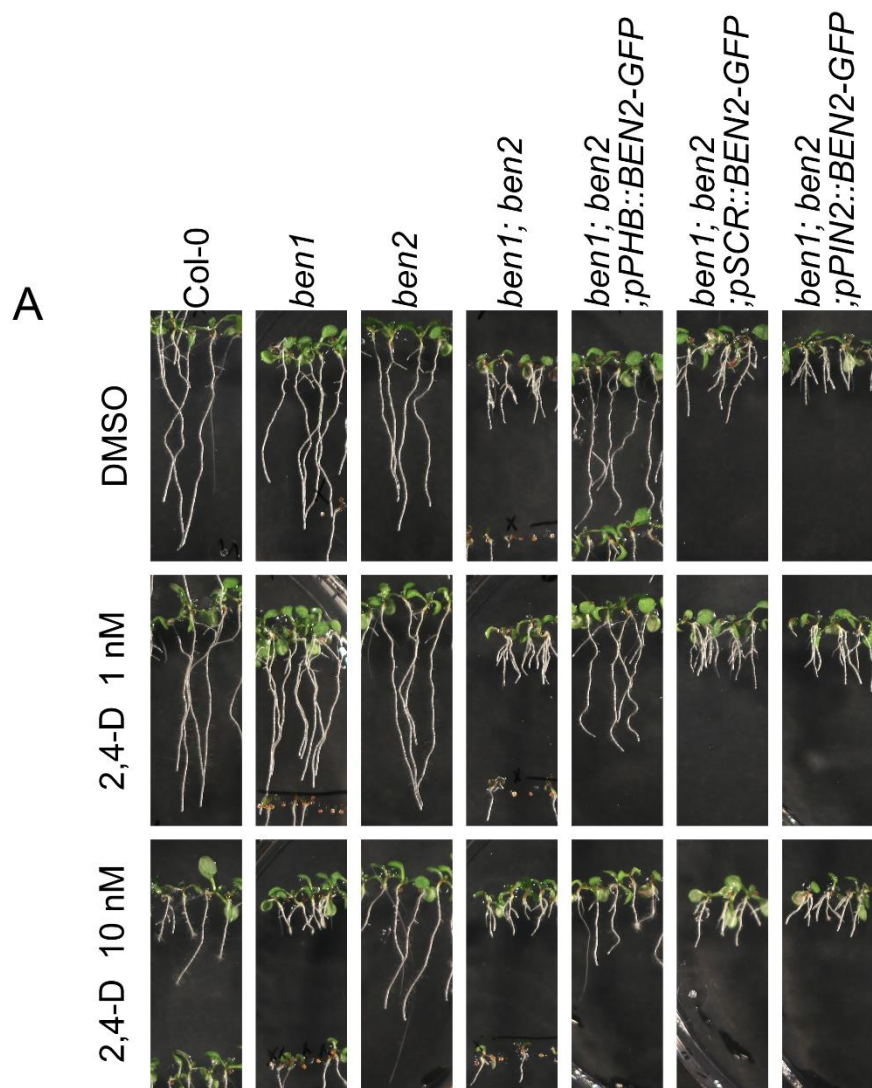


**Figure 10. Phenotypes of transgenic plants expressing *BEN2/VPS45-GFP* under control of tissue-specific promoters treated with 2,4-D.**

(A, B) Seedlings (A) and root length (B) of mutants and transgenic lines at 7 DAG treated with DMSO (upper images), 1 nM 2,4-D (middle images), and 10 nM 2,4-D (lower images). (B) At least two independent experiments resulted in similar results. Error bars indicate SD ( $n \geq 23$ ). Results of statistic evaluation was shown as follows:  $0.01 < p\text{-value} \leq 0.05$  (\*);  $p\text{-value} \leq 0.01$  (\*\*) and not significant (ns). The treatment effects were different between the mutants with statistically significance, which was assessed using two-way ANOVA. Scale bar: 10 mm in (A).

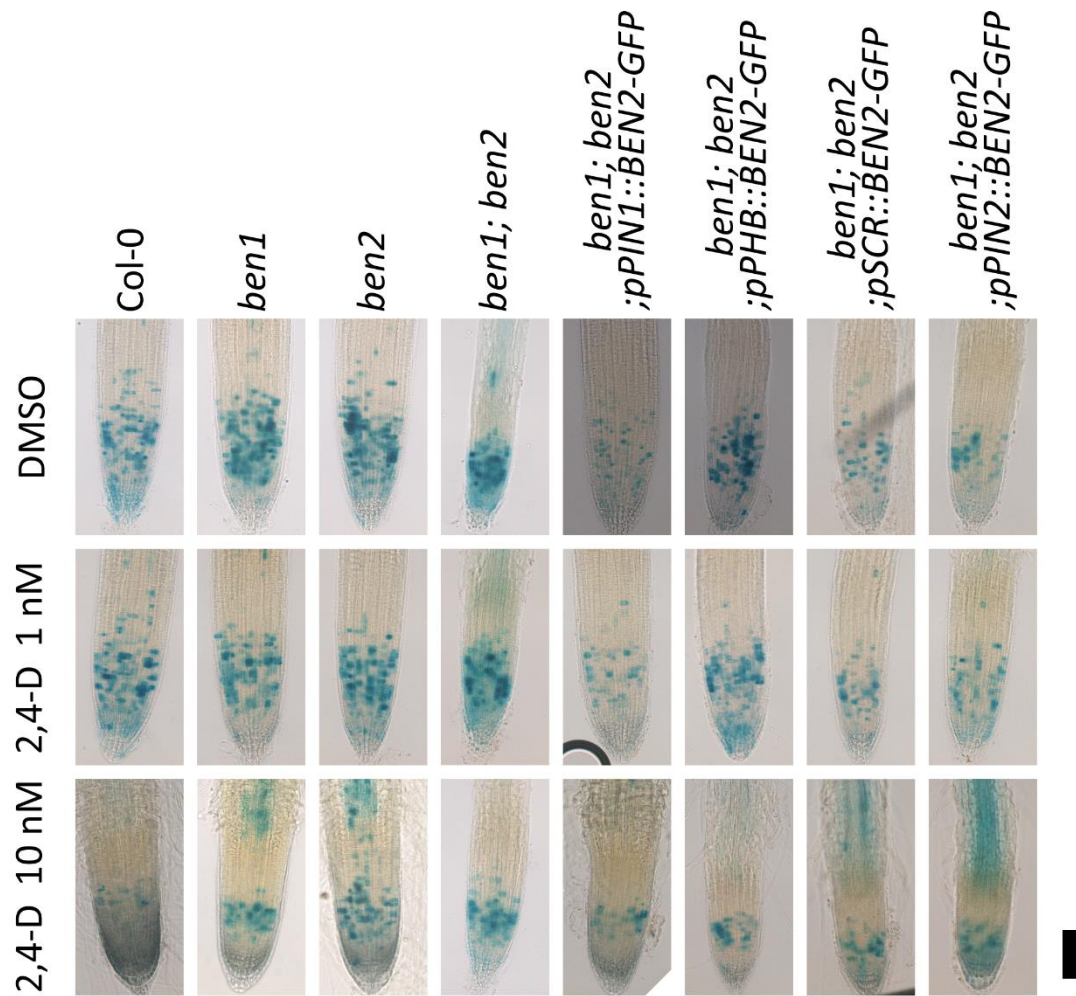


**Figure 11. Expression patterns of *CycB1;1-GUS* in transgenic lines expressing *BEN2/VPS45-GFP* driven by tissue-specific promoters treated with 2,4-D.**

Expression patterns of *CycB1;1-GUS* in *CycB1;1-GUS*, *ben1; CycB1;1-GUS*, *ben2; CycB1;1-GUS*, *ben1; ben2; CycB1;1-GUS*, *ben1; ben2; pPIN1::BEN2-GFP; CycB1;1-GUS*, *ben1; ben2; pPHB::BEN2-GFP; CycB1;1-GUS*, *ben1; ben2; pSCR::BEN2-GFP; CycB1;1-GUS*, and *ben1; ben2; pPIN2::BEN2-GFP; CycB1;1-GUS* seedlings at 7 DAG. Seedlings were treated with DMSO (upper images), 1 nM 2,4-D (middle images), and 10 nM 2,4-D (lower images). Scale bar: 100  $\mu$ m.

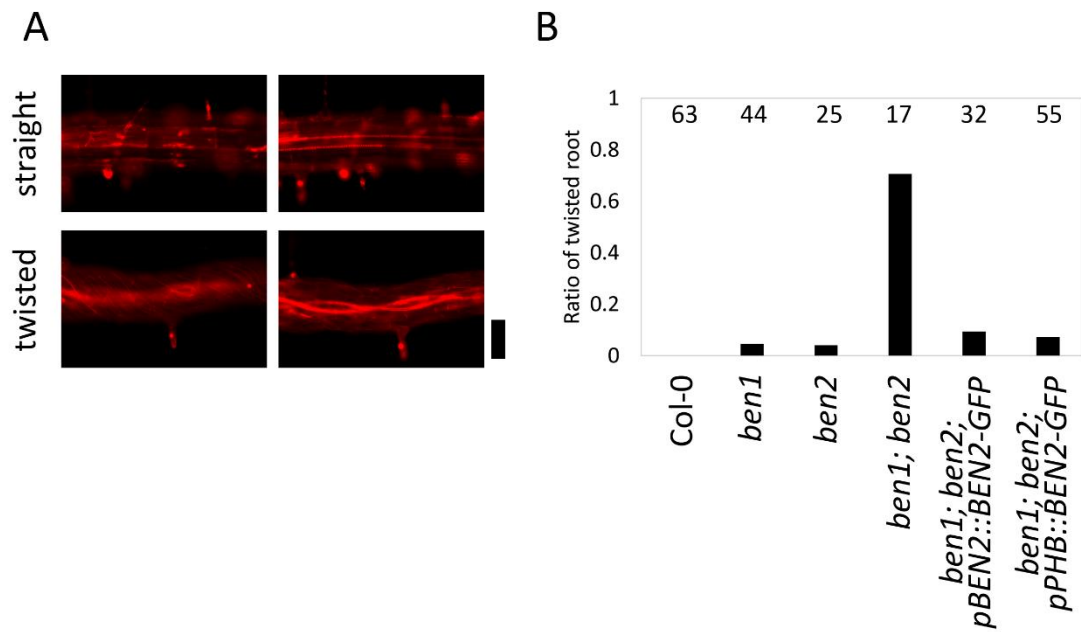


**Figure 12. The ratio of twisted root in transgenic lines expressing *BEN2/VPS45-GFP* driven by tissue-specific promoters.**

(A) Straight (upper) and twisted (lower) root tip. Left images show the root epidermal cells and right images show the inner side of root. (B) The ratio of twisted roots in Col-0, *ben1*, *ben2*, *ben1; ben2*, *ben1; ben2; pBEN2::BEN2-GFP*, and *ben1; ben2; pPHB::BEN2-GFP*. Scale bar: 100  $\mu$ m.

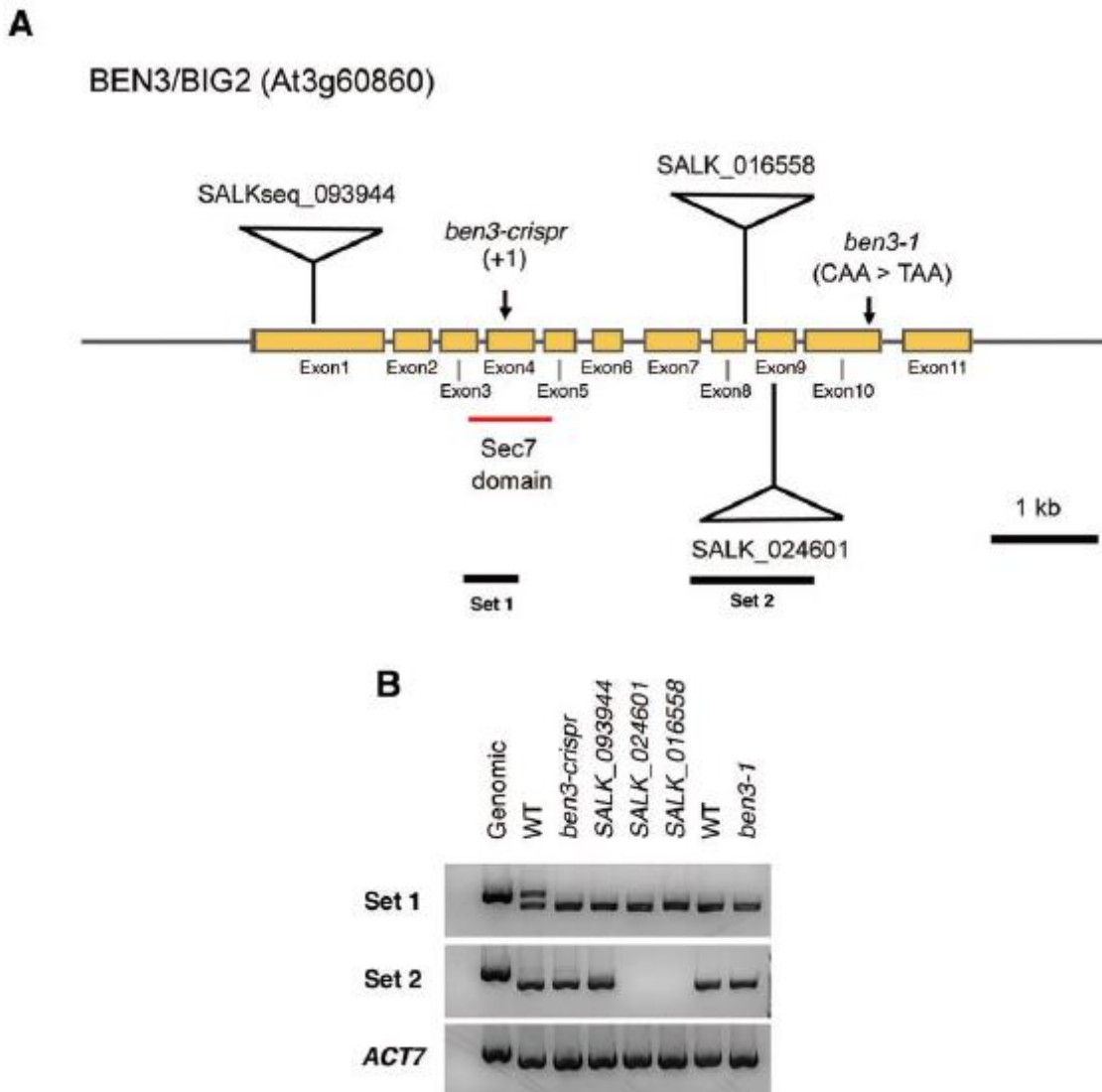


**Figure 13. Sites of *big2* mutations and transcript accumulation.**

(A) Relative positions of mutations in the *BEN3/BIG2* gene. Coding regions were indicated by orange boxes. Set 1 and Set 2 indicate the regions examined by RT-PCR. T-DNAs were not drawn in scale. (B) Characterization of *BEN3/BIG2* transcript accumulation in the mutants by RT-PCR. Set 1 and Set 2 represent different primer sets to amplify parts of *BEN3/BIG2* cDNA.

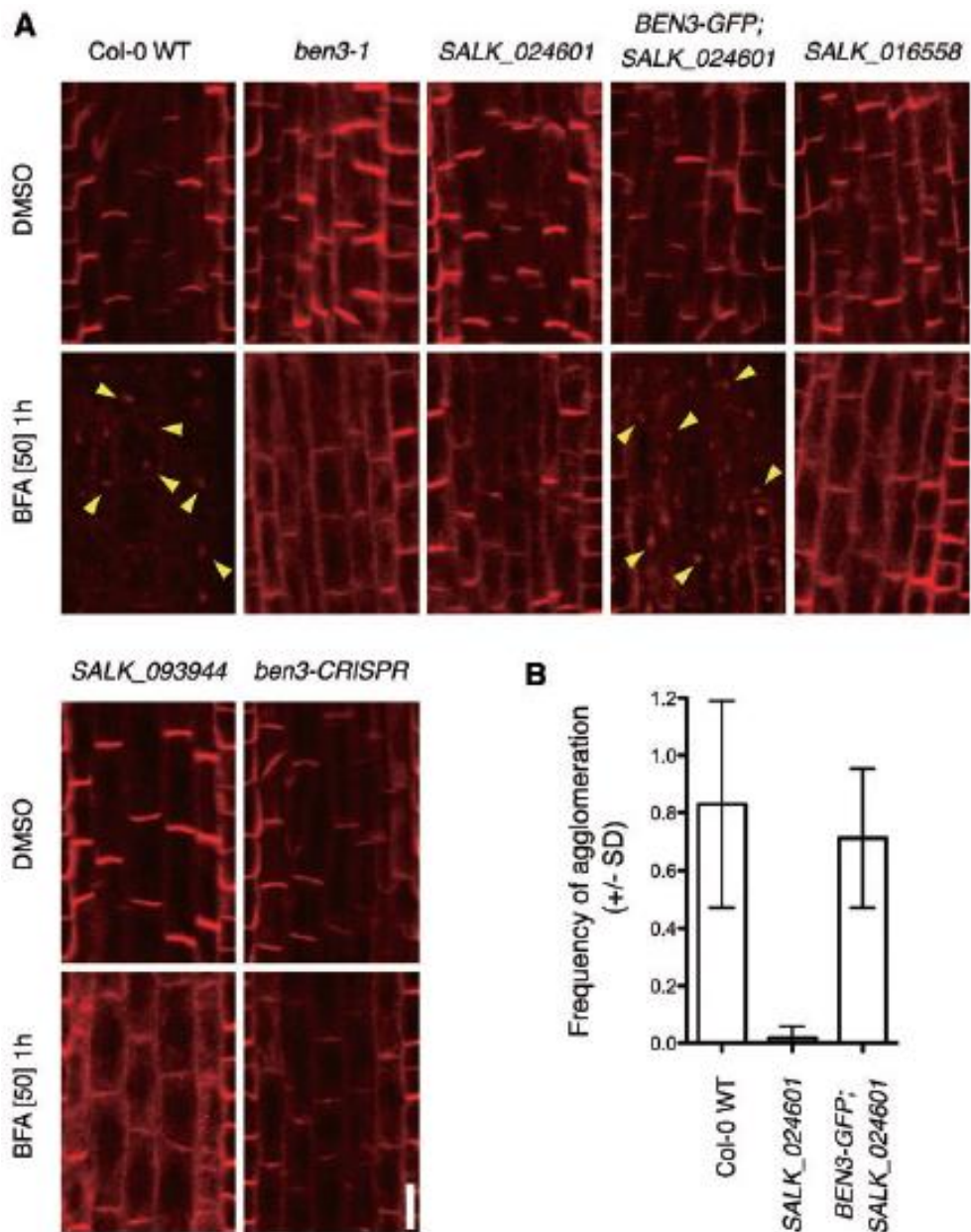


**Figure 14. *ben3* and *big2* mutants exhibit PIN1 relocation defects.**

(A) Anti-PIN1 immunostaining of wild-type, *ben3* and *big2* alleles. BFA treatment (50 mM, 1 h) caused intracellular accumulation of PIN1 in wild-type root vasculature (arrowheads), whereas *ben3-1* and *big2* homozygous mutants (*SALK\_016558*, *SALK\_024601*, *SALK\_093944* and *ben3-CRISPR*) had less pronounced intracellular PIN1 agglomeration. In the *SALK\_024601* homozygous seedlings containing the *pBEN3::BEN3-GFP* construct, BFA induced clear PIN1 agglomeration as in the wild type (arrowheads). Scale bar = 10 mm. (B) Quantitative evaluation of intracellular PIN1 signals. Frequencies of the agglomerated PIN1 signals from the wild type, the *big2* homozygous mutant (*SALK\_024601*) and the mutant harboring the *BEN3-GFP* transgene (*BEN3-GFP; SALK\_024601*) are presented with the SD. The P-values obtained from Mann–Whitney test were: Col-0 (wild type vs. *SALK\_024601*, P = 0.0013; *SALK\_024601* vs. *BEN3-GFP; SALK\_024601*, P = 0.0019; Col-0 (wild type) vs. *BEN3-GFP; SALK\_024601*, P = 0.3582.

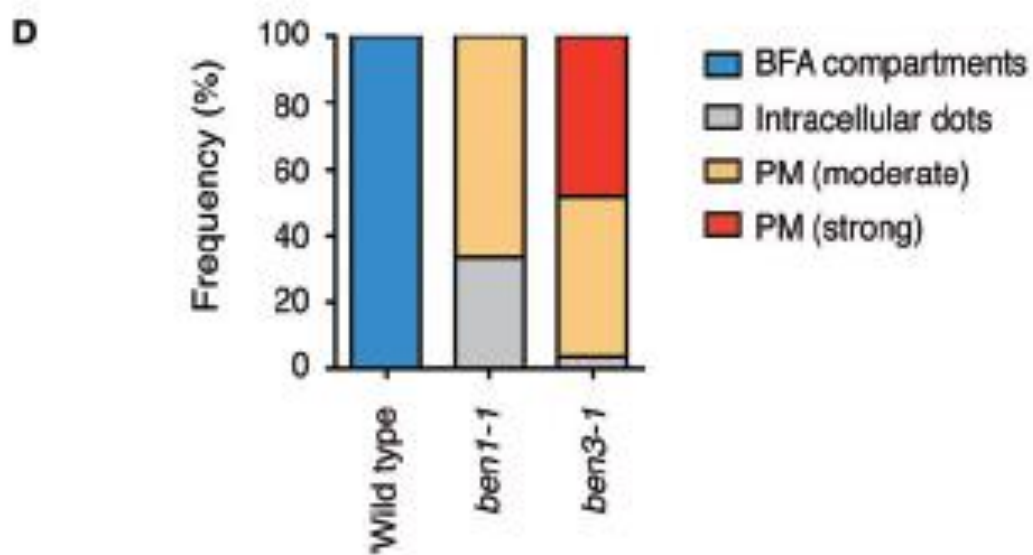
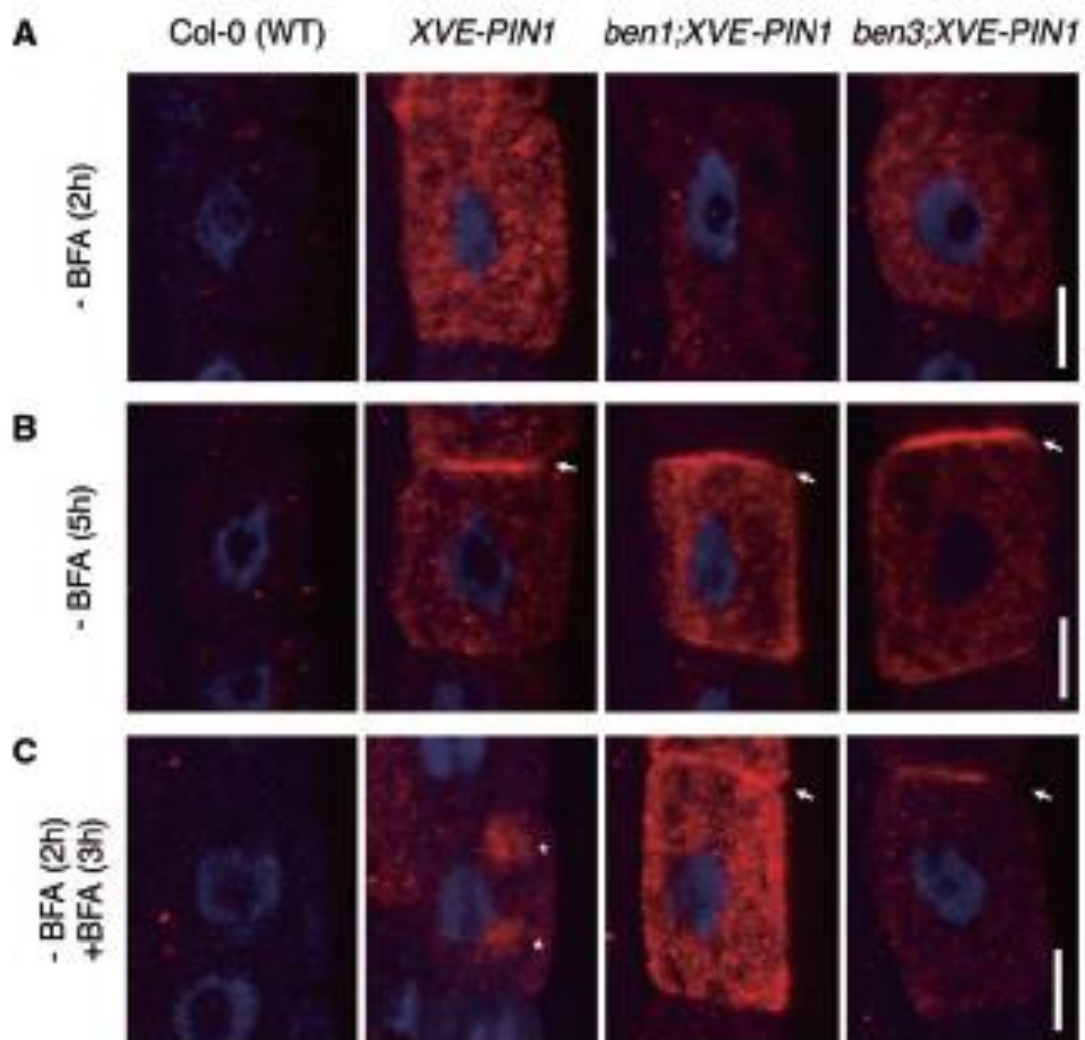


**Figure 15. *ben3* mutation affects BFA-sensitive trafficking of PIN1 to the plasma membrane.**

(A, B) The wild type (Col-0), XVE-PIN1 on the wild-type, *ben1-1* and *ben3-1* background treated with b-estradiol (1 mM, 5 min) and incubated in 1/2 MS medium for 2 h (A) or 5 h (B) were immunostained with anti-PIN1 antibody (red) and stained with 40,6-diamidino-2-phenylindole (DAPI; blue). Arrows indicate PM-localized PIN1 signals. (C) Seedlings incubated for 2 h in 1/2 MS medium after the b-estradiol treatment (1 mM, 5 min) and subsequently in BFA-containing medium (25 mM, 3 h). Asterisks indicate intracellular accumulation of PIN1 signal in an epidermal cell of the XVE-PIN1 on the wild-type background. (D) Quantification of PIN1 localization in BFA-treated root epidermal cells. Estradiol-induced PIN1 predominantly localized at the BFA compartment in the wild-type background (22/22 cells). In the *ben1-1* background, comparable levels of PIN1 signals were often detected both at the PM and as intracellular dots (orange, 24/36 cells), whereas stronger PM localization of PIN1 was frequently observed in the *ben3-1* mutant background (red, 14/29 cells). Scale bars = 10  $\mu$ m.

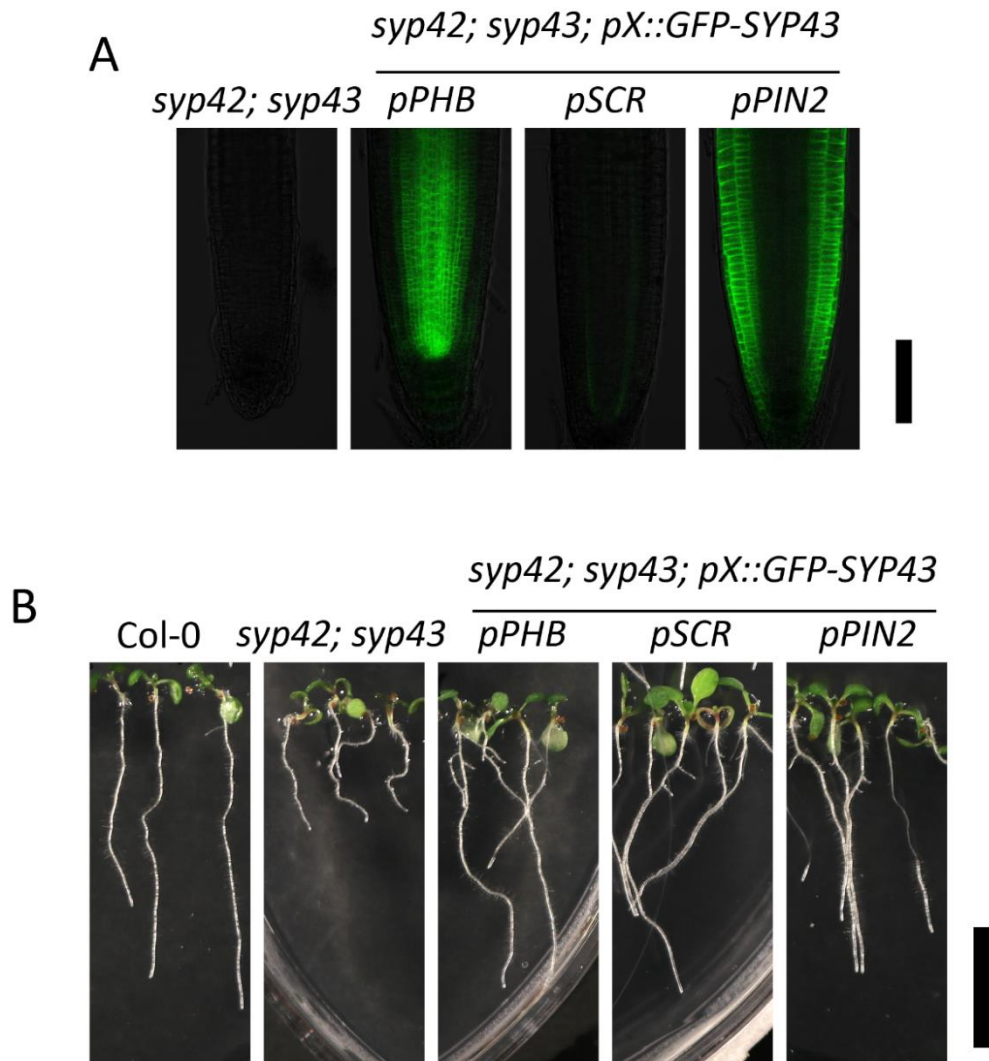


**Figure 16. Phenotypes of transgenic plants expressing *GFP-SYP43* under control of tissue-specific promoters.**

(A) Expression of *GFP-SYP43* on the *syp42; syp43* double mutant background. Whereas *GFP-SYP43* expressed under *PHB* promoter was mainly detected in stele, *GFP* was detected mainly in QC and endodermis in *pSCR::GFP-SYP43* and in the outer tissues in *pPIN2::GFP-SYP43* lines. Note that *syp42; syp43* double mutant which does not harbor *GFP* has faint autofluorescence. (B) Seedlings of mutants and transgenic lines at 7 DAG. Scale bars: 100  $\mu$ m in (A) and 10 mm in (B).

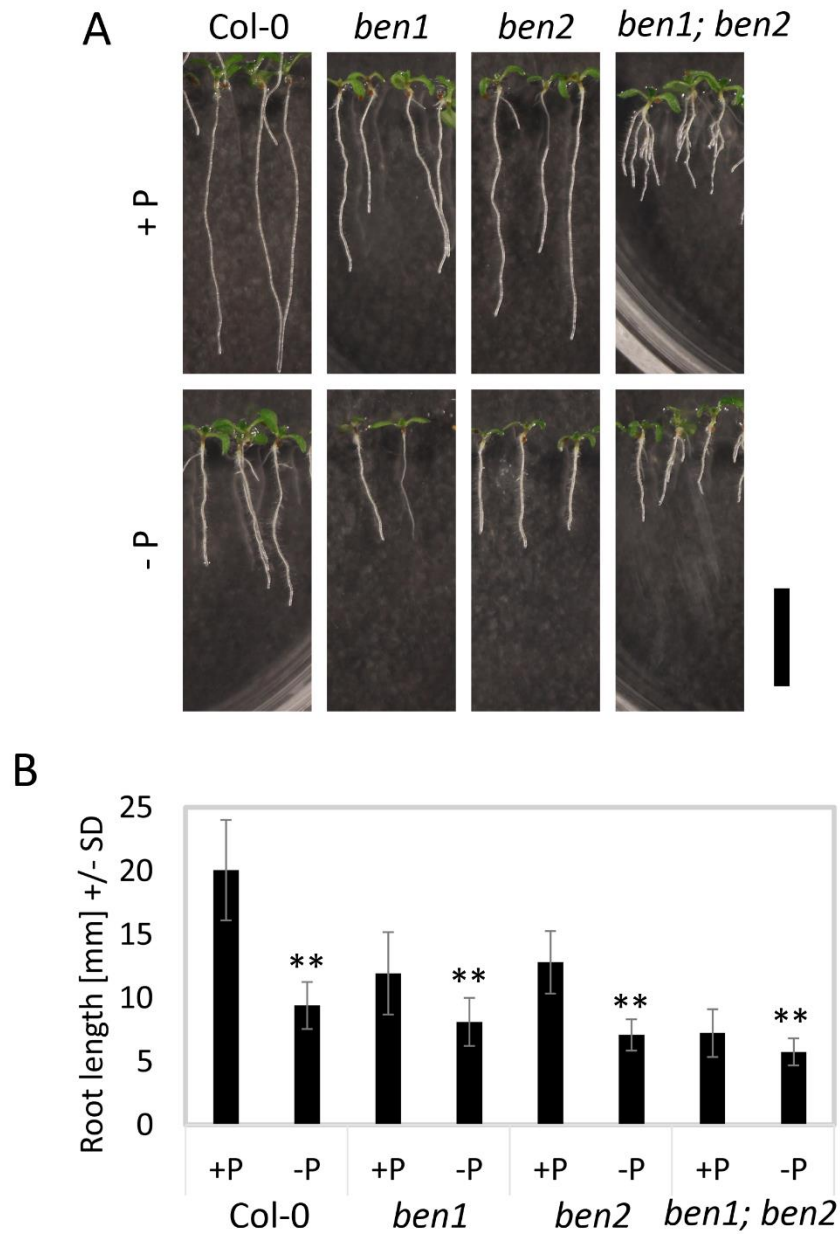


**Figure 17. Phenotypes of mutants under phosphate starvation.**

(A, B) Seedlings (A) and root length (B) of mutants at 7 DAG grown on the normal media (upper images) and phosphate starvation media (lower images). (B) At least three independent experiments resulted in similar results. Error bars indicate SD ( $n \geq 49$ ). Results of statistic evaluation was shown as follows:  $0.01 < p\text{-value} \leq 0.05$  (\*);  $p\text{-value} \leq 0.01$  (\*\*) and not significant (ns). Scale bar: 10 mm in (A).

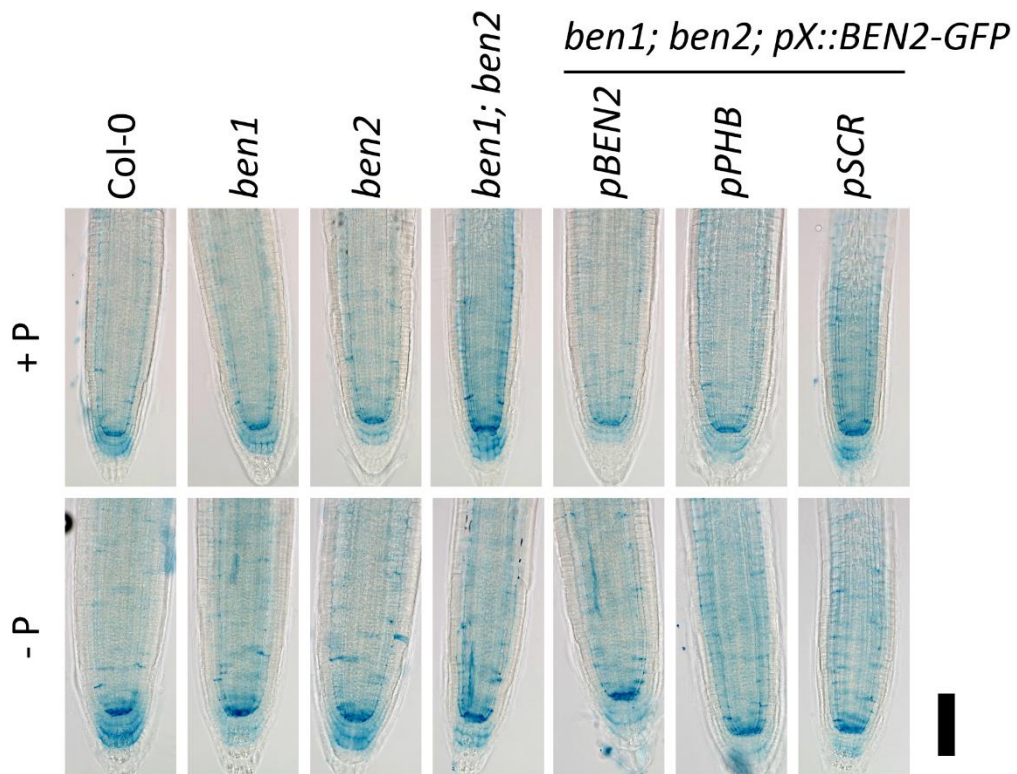


**Figure 18. Iron deposition patterns under the phosphate starvation condition.**

The root tips of Col-0, *ben1*, *ben2*, *ben1; ben2*, *ben1; ben2; pBEN2::BEN2-GFP*, *ben1; ben2; pPHB::BEN2-GFP*, and *ben1; ben2; pSCR::BEN2-GFP* on the normal media (upper images) and phosphate starvation media (lower images) at 5 DAG. Iron deposition (blue) was detected with Perls staining. Scale bar: 100  $\mu$ m.

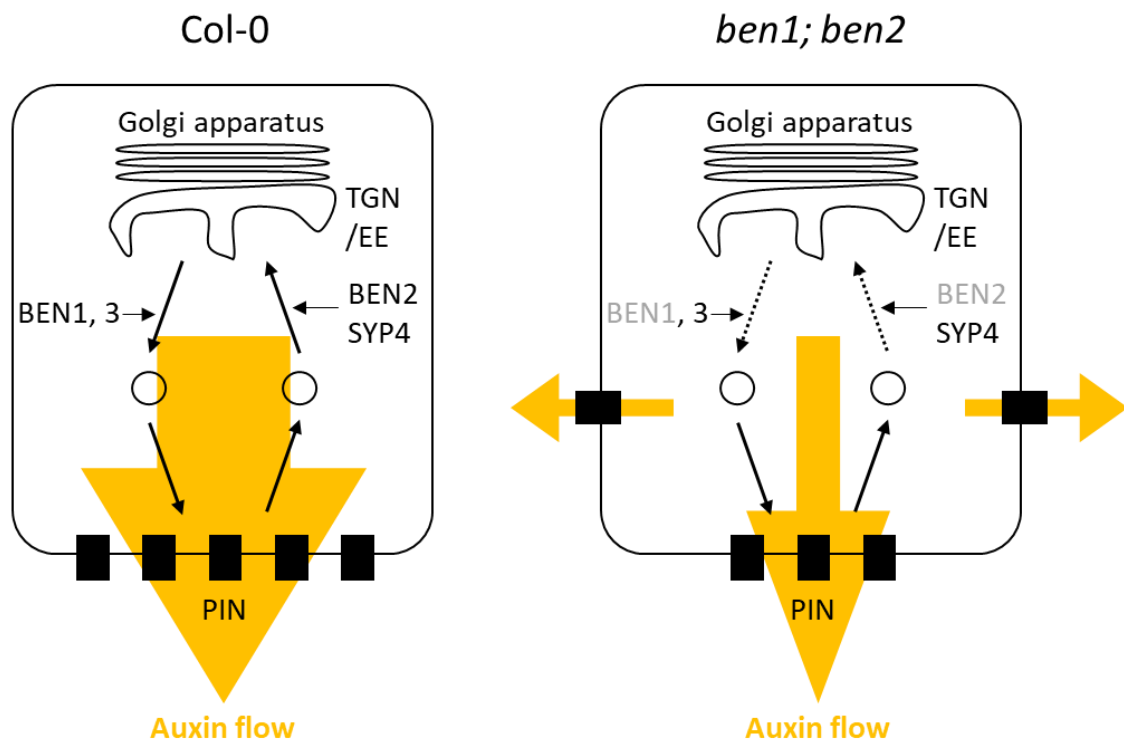


**Figure 19. The mutation in *BEN1* and *BEN2* results in the defect of auxin distribution**

When the function of *BEN1* and *BEN2* involved in the transport from TGN/EE to PM is impaired, PIN proteins are not transported to the proper compartment of PM. This results in the leak of auxin to wrong direction, leading in the alteration of auxin distribution in individual level.

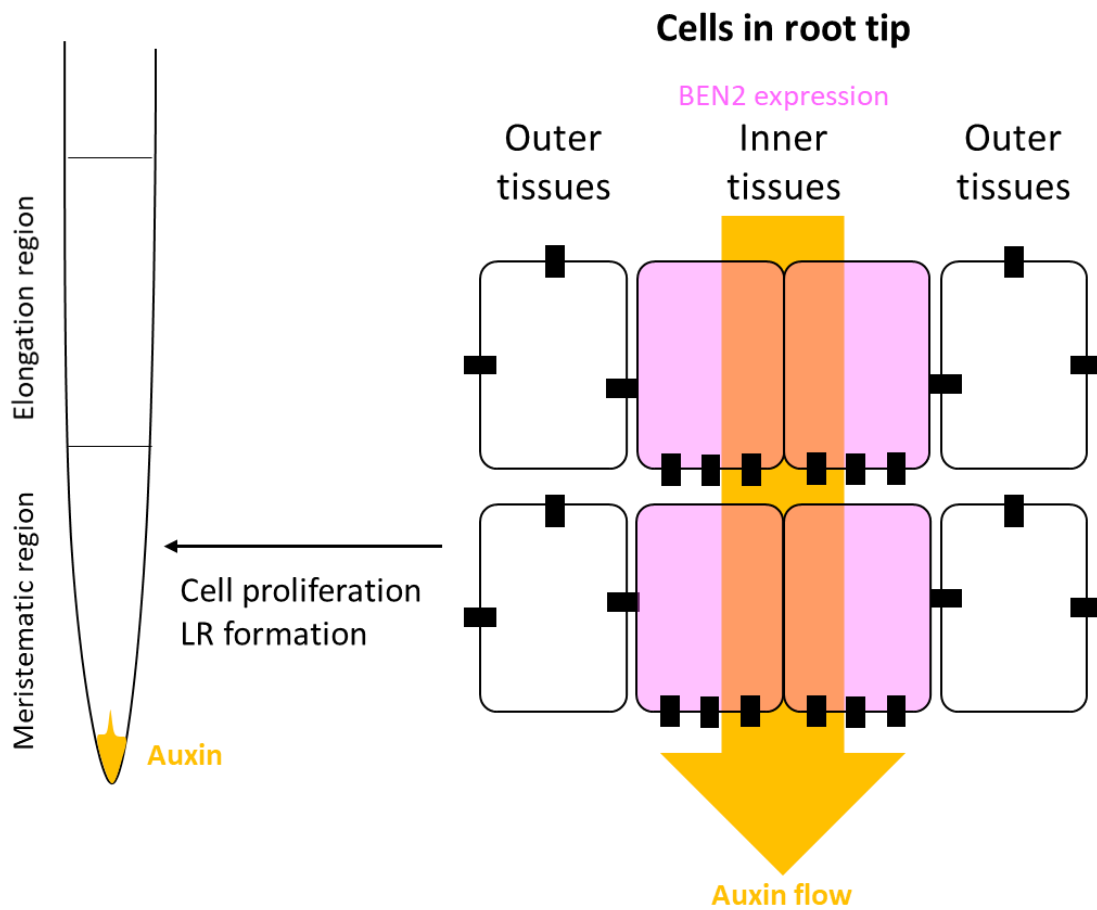


**Figure 20. BEN2 expressed in inner tissues is required for root elongation and lateral root formation**

BEN2 expressed in inner tissues results in the recovery of PIN polarity and auxin distribution in *ben1; ben2* root tip, which is sufficient to keep cell proliferation and form lateral roots.